

Surface deformation during a magmatic intrusion : the example of the Dabba'hu rift crisis of 2005-2007 (Afar, Ethiopia)

Raphaël Grandin*, Anne Socquet*, Renaud Binet✦, Eric Jacques*, Yann Klinger*, Jean-Bernard de Chabaliér*, Geoffrey King*, Stephen Tait*, Paul Tapponnier*, Arthur Delorme*, Célia Elissalde* & Paul Pinzuti*



Institut de Physique du Globe de Paris



Commissariat à l'Énergie Atomique

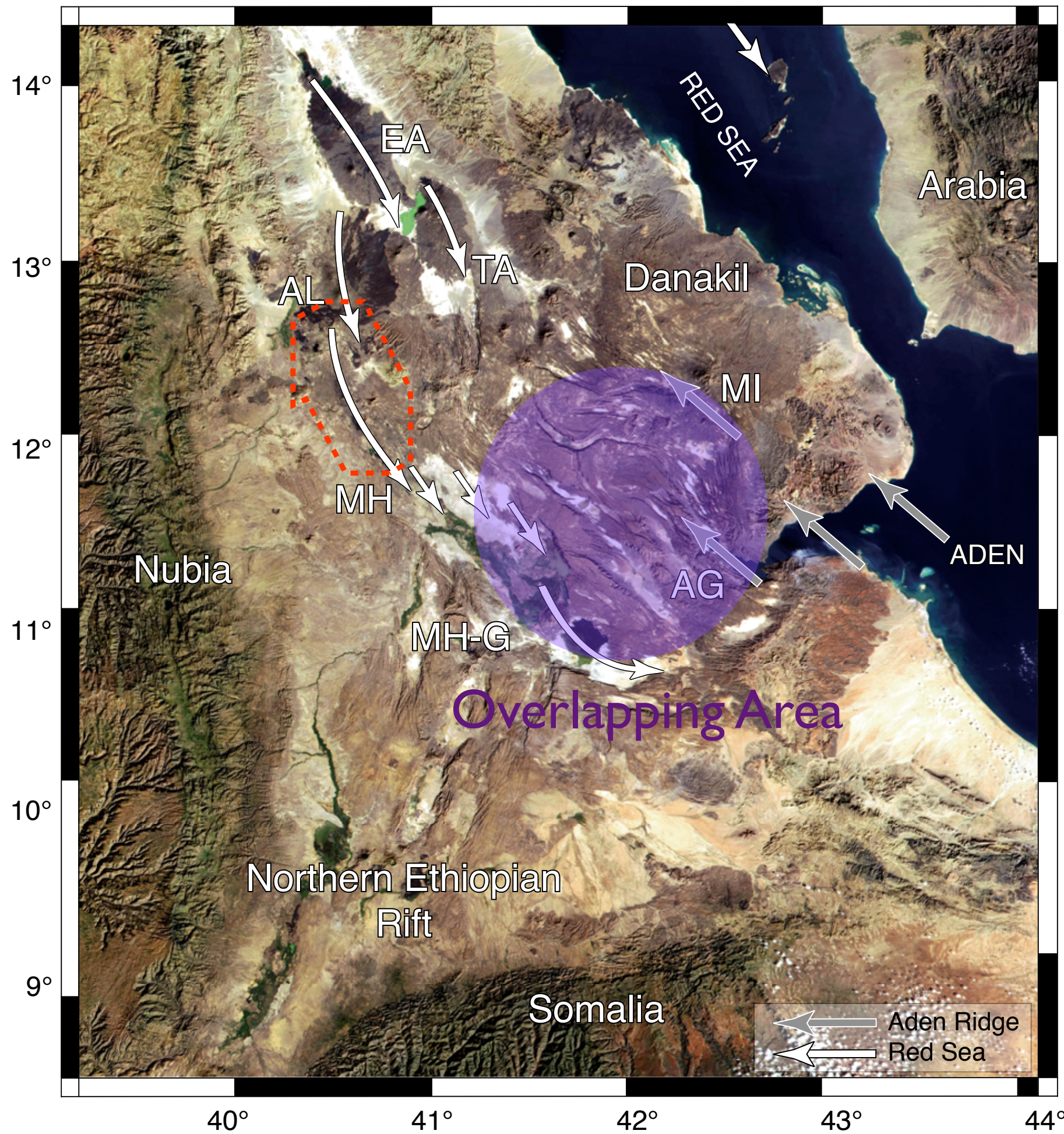
Atalay Ayele (Geoph. Obs., Addis)

Cécile Lasserre & Marie-Pierre Douin (ENS, Paris)

Cécile Doubre (IPGS, Strasbourg)

Cindy Ebinger (Rochester University, NY)

Mark Simons (CalTech)



Tectonic setting

- A system of overlapping rifts, forming two groups:
- Red Sea - Erta Ale - Alayta - Manda Hararo - Goba'ad
 - Aden - Ghoubbet - Asal - Manda Inakir

Extension rate across Afar:
 ~ 1.5 cm/year (Vigny *et al.*, 2006)

Extension rate across Dabba'hu rift:
 ~ 1.0 cm/year

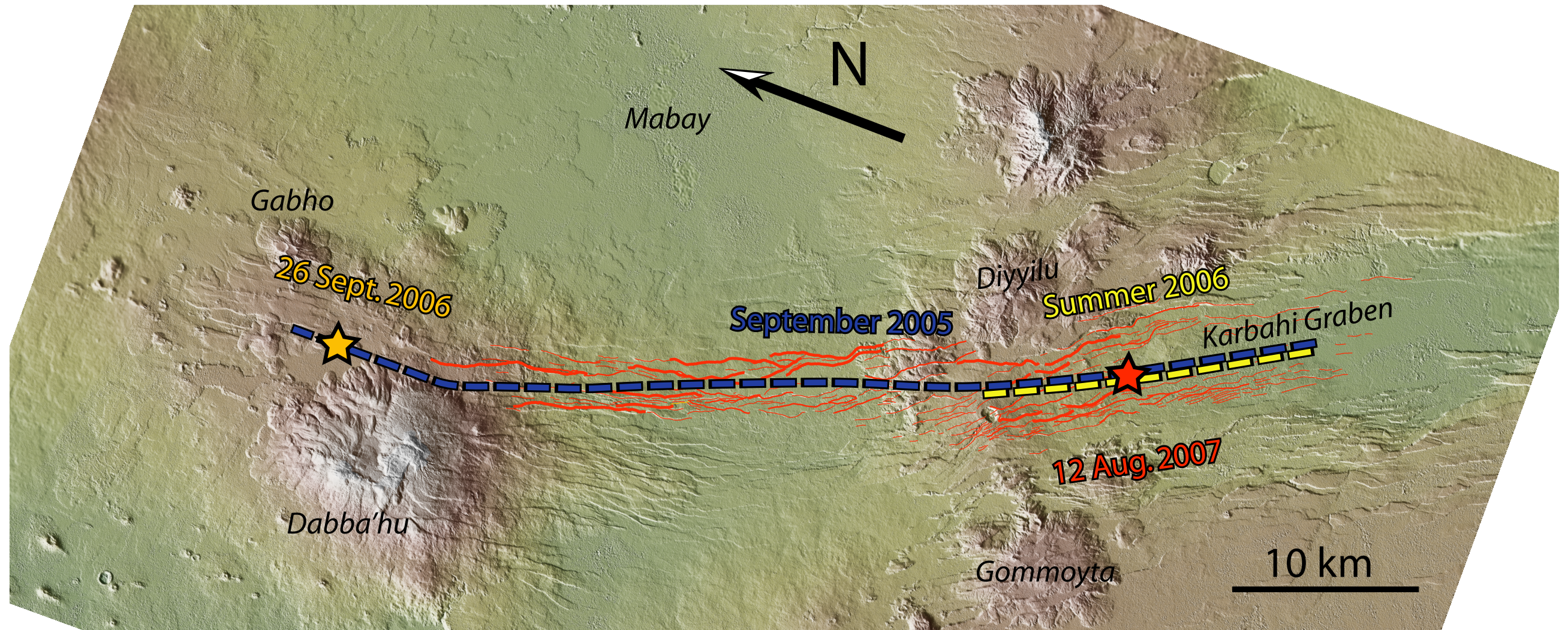
Amount of extension during the crisis (co + post):
 ~ 5-10 m

⇒ One similar event every
 500-1000 years?

Arrows modified from Manighetti *et al.* (1998) and Pinzuti (2006)

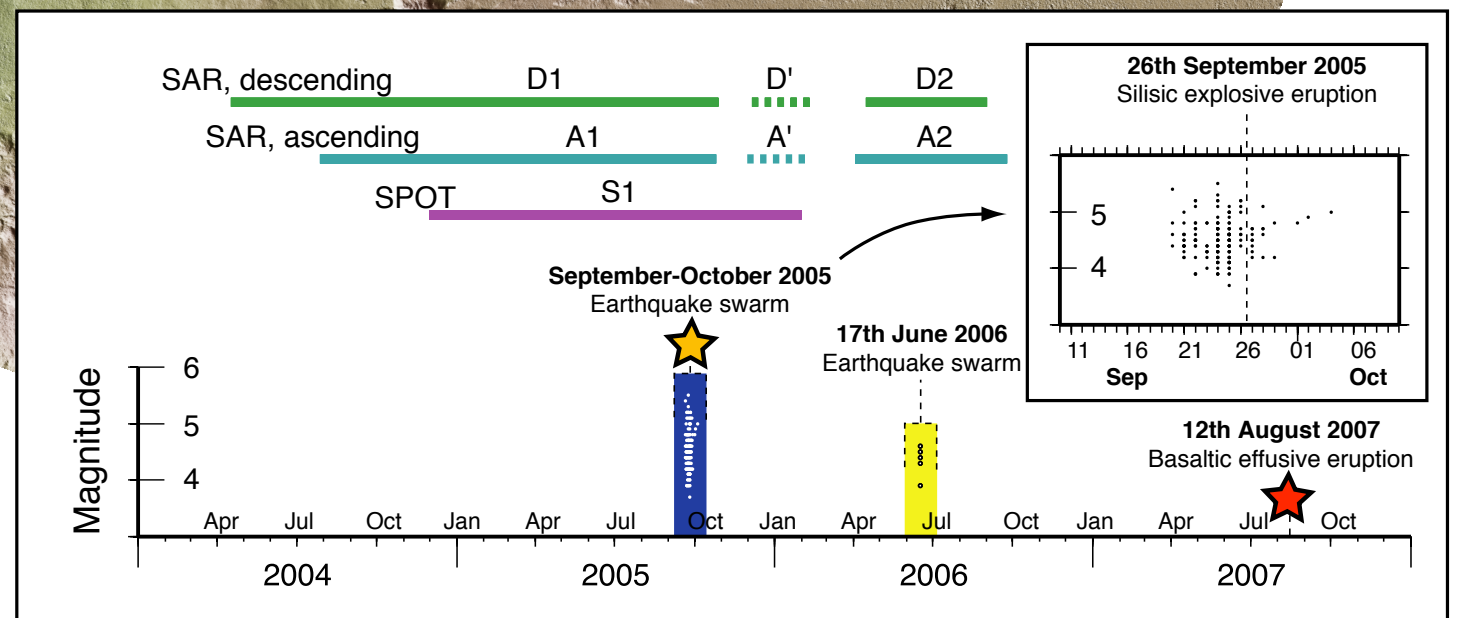
Landsat mosaic from Pinzuti (2006)

Location of the main intrusive and eruptive events within the Dabba'hu rift

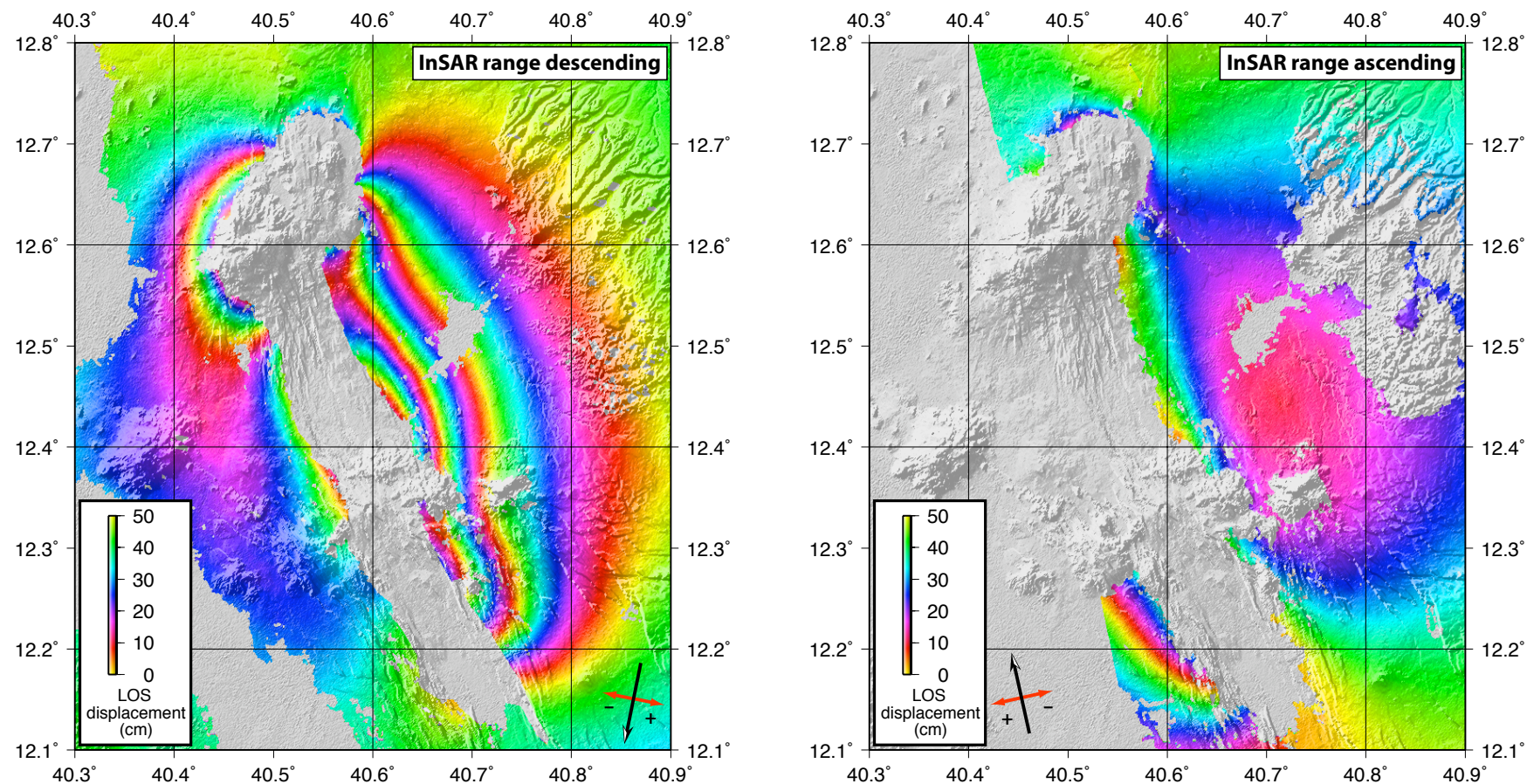


In red: faults mapped using InSAR images D' and A' (late november 2005 to early February 2006)

20 m DEM, generated with SPOT images



InSAR data



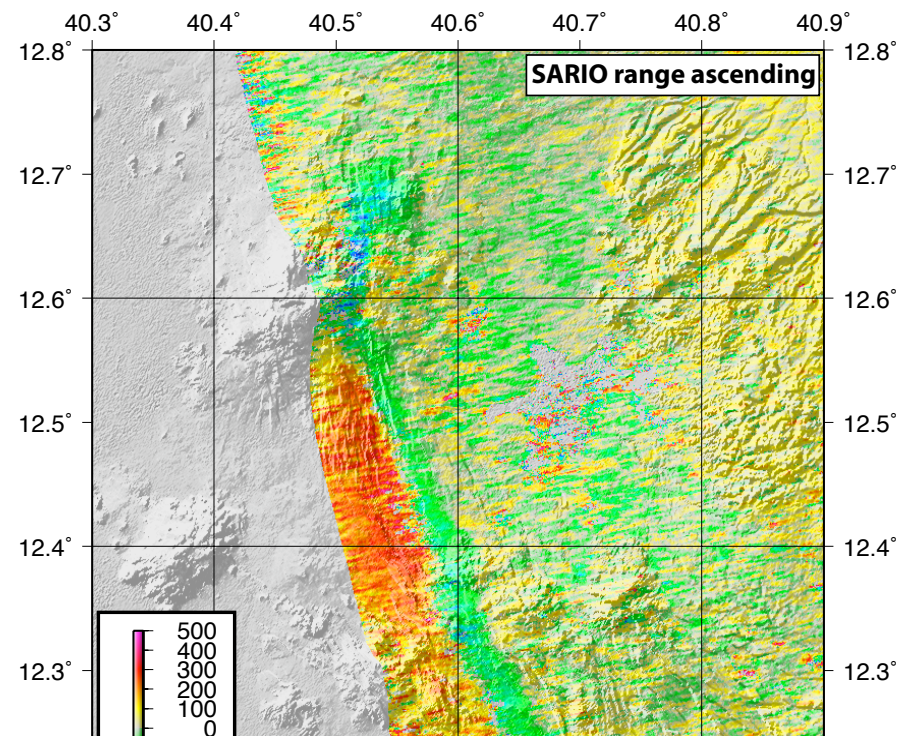
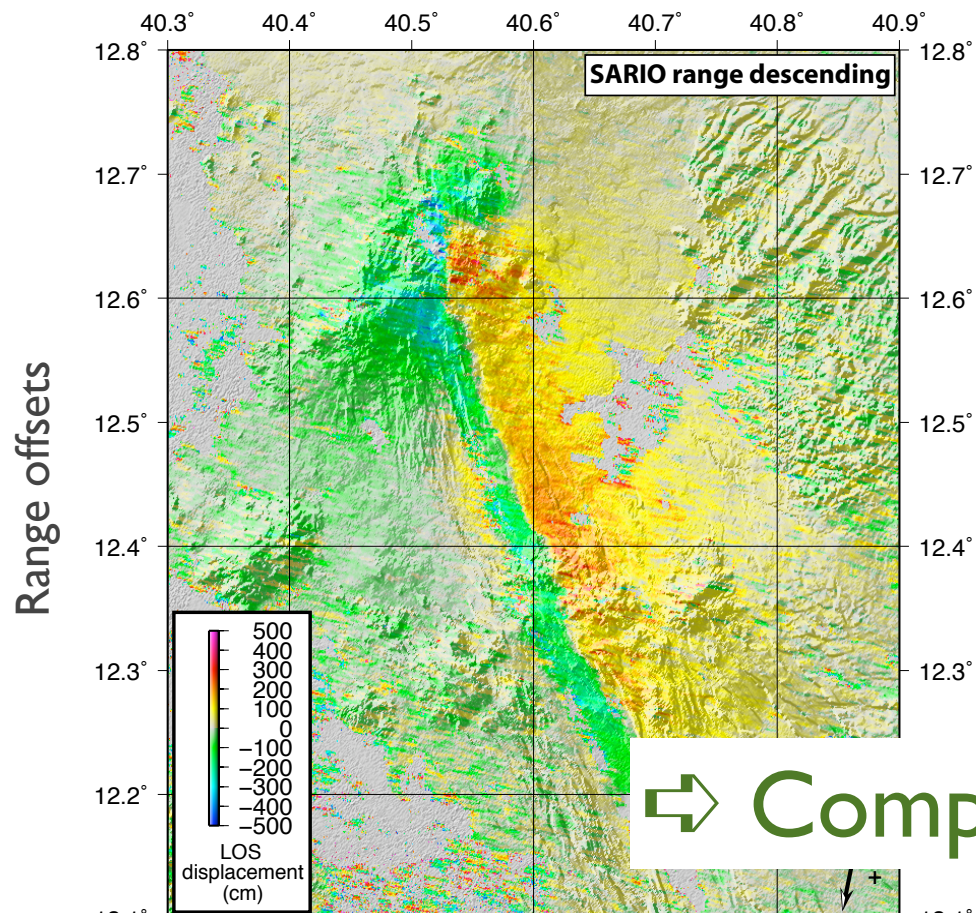
- Very accurate measurement (precision: ~ 1 cm)
- Mostly sensitive to the vertical component of surface displacement
- Ascending and descending tracks can be combined to separate vertical and horizontal components, if we make a kinematic hypothesis (e.g. displacement is rift perpendicular)
- Unwrapping is only possible in the far field: we cannot reach the rift floor

⇒ Provides a very good constraint on opening at depth

SARIO data

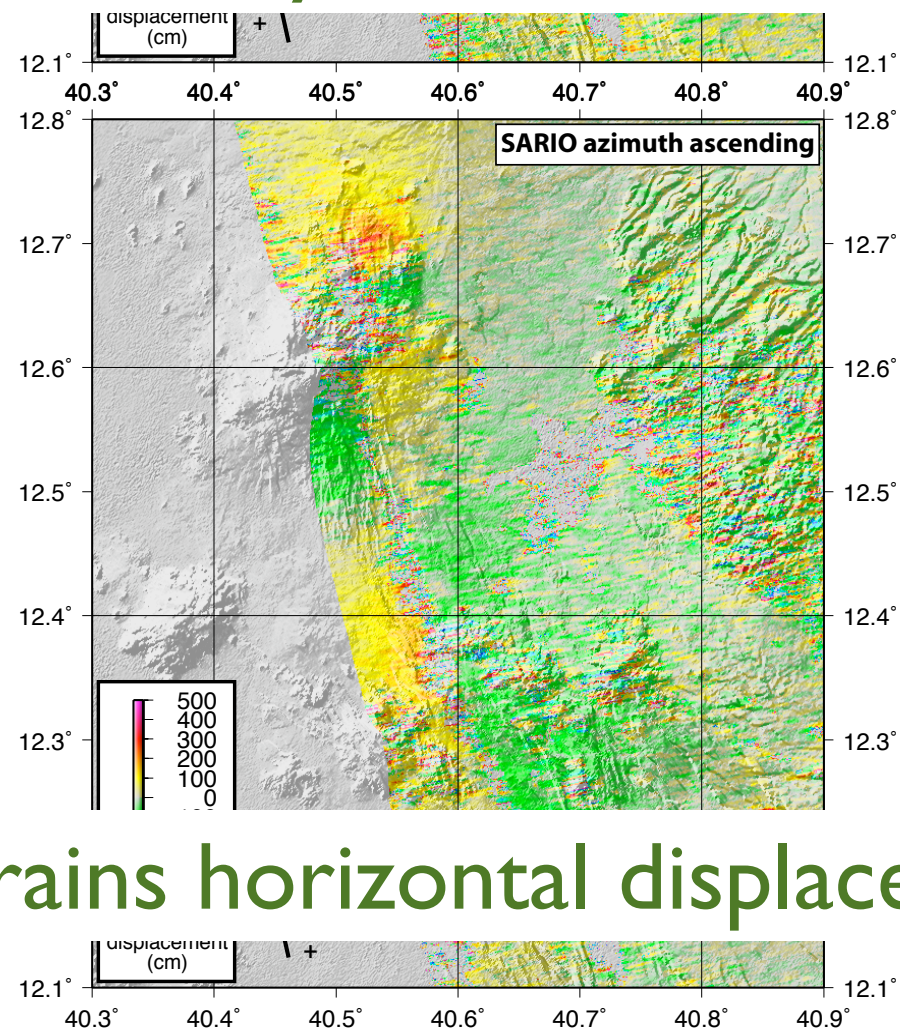
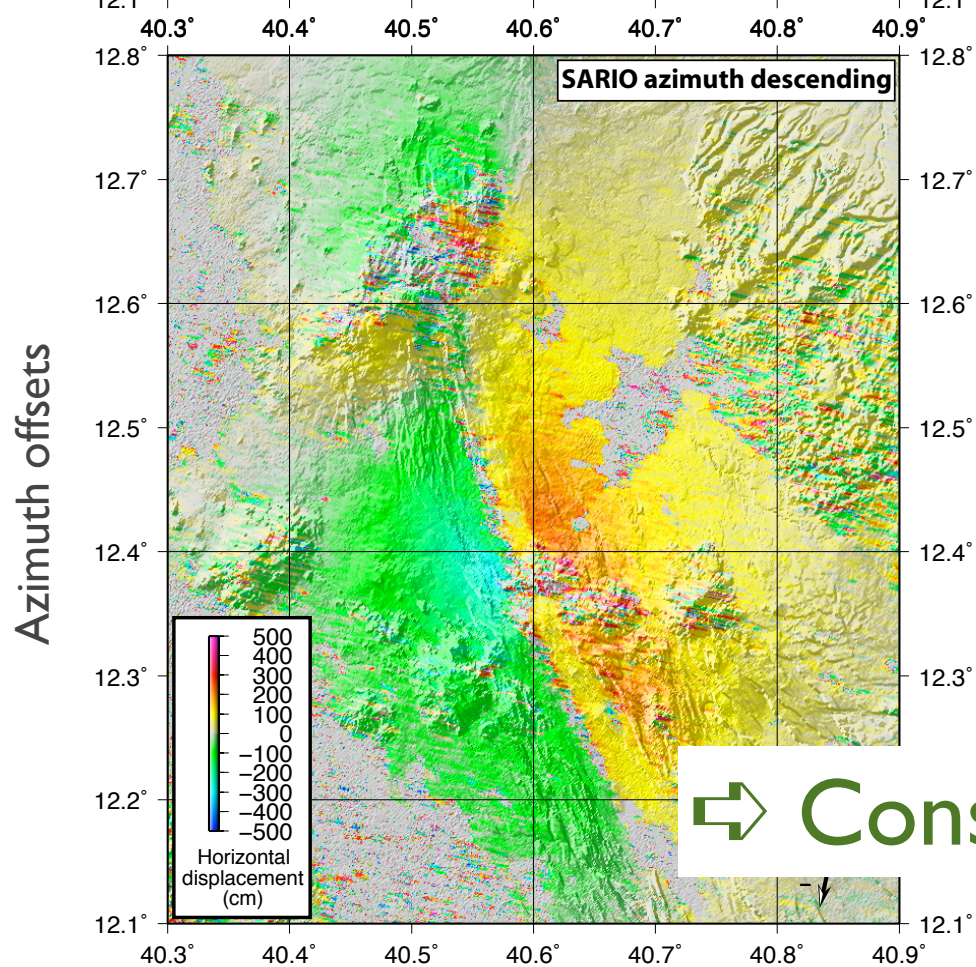
Descending track

Ascending track



- Accuracy ~ 50 cm
- Same geometry as InSAR

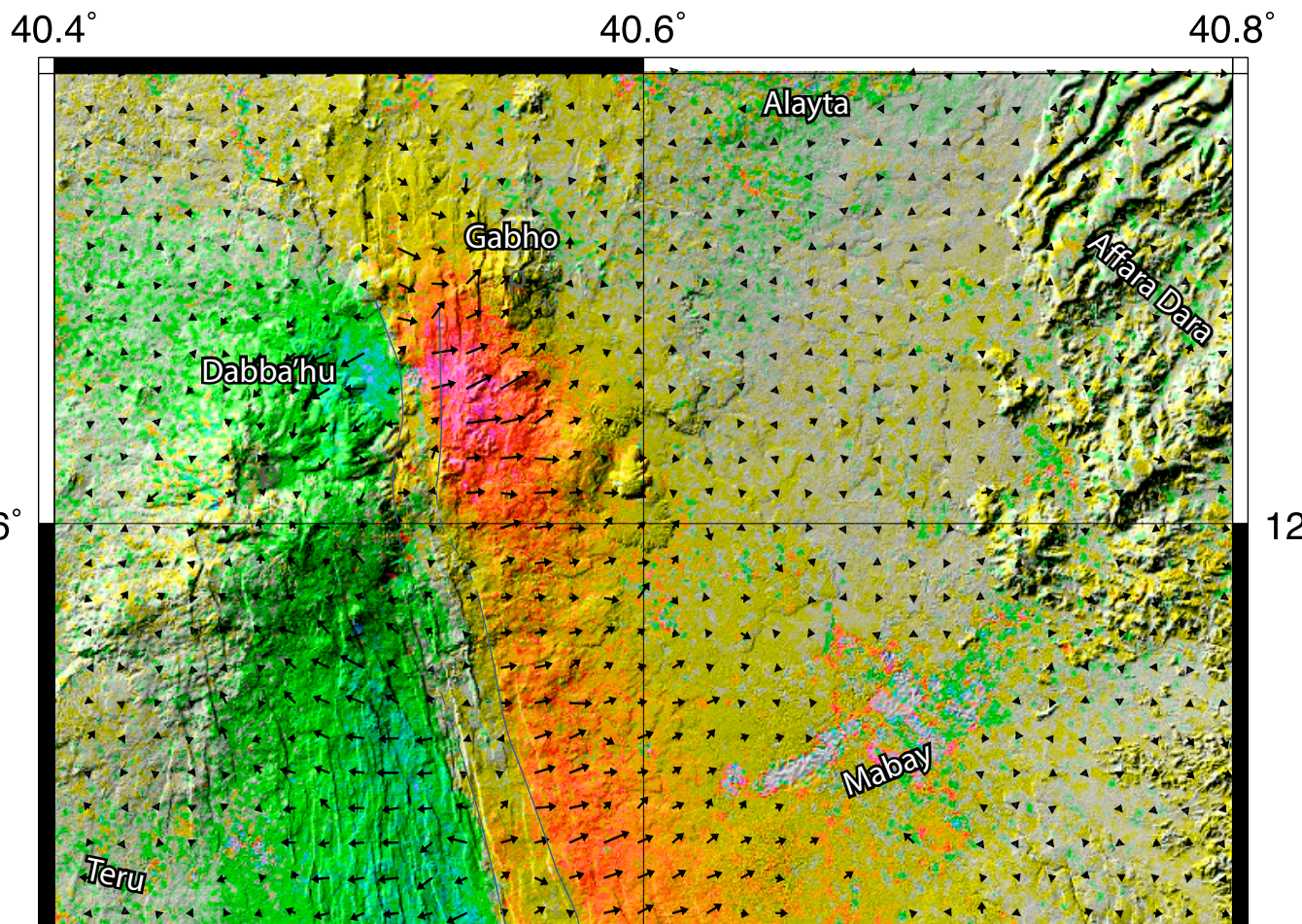
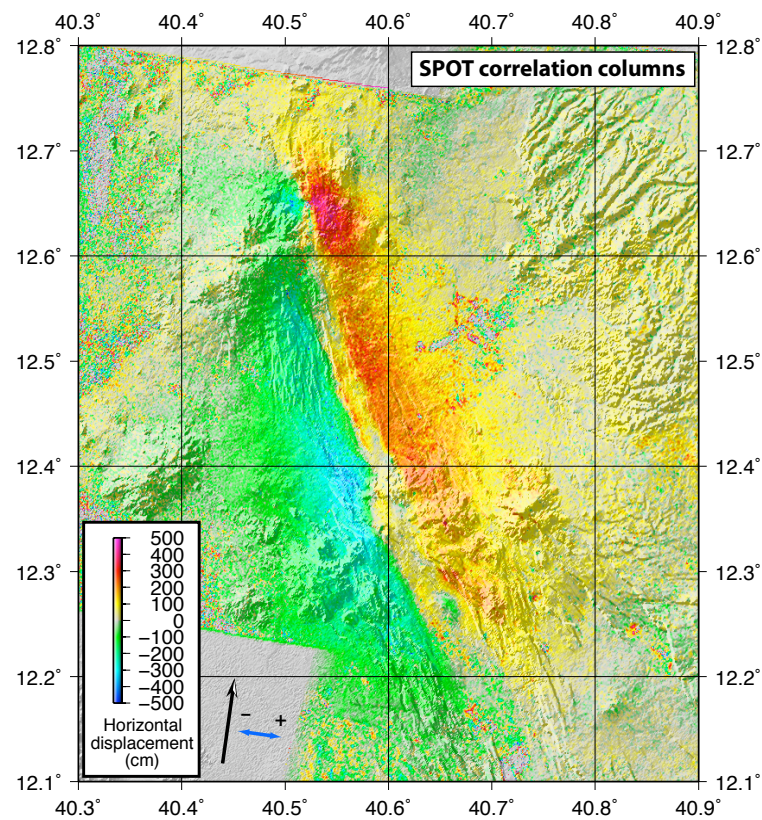
⇒ Complementary of InSAR in the near-field



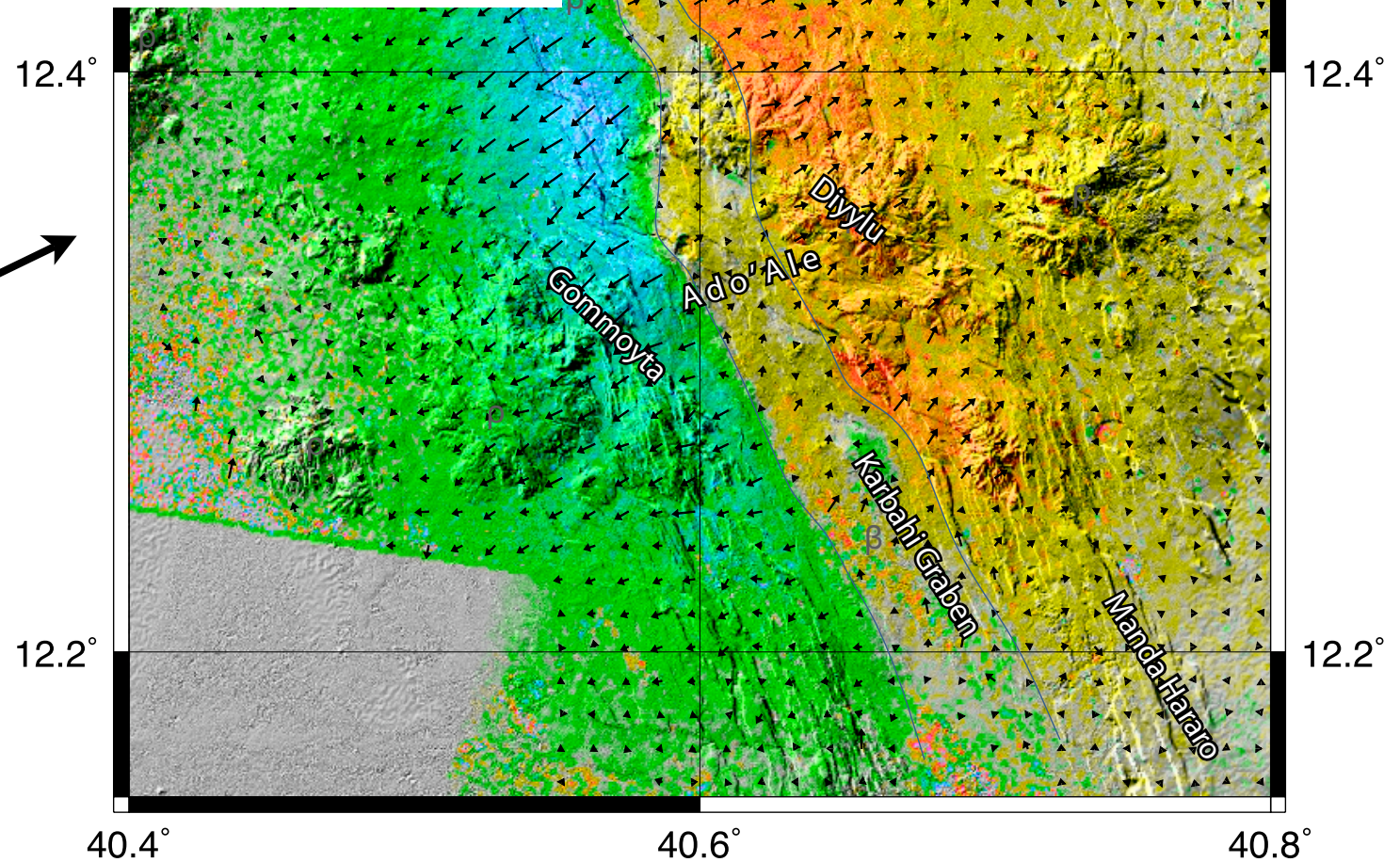
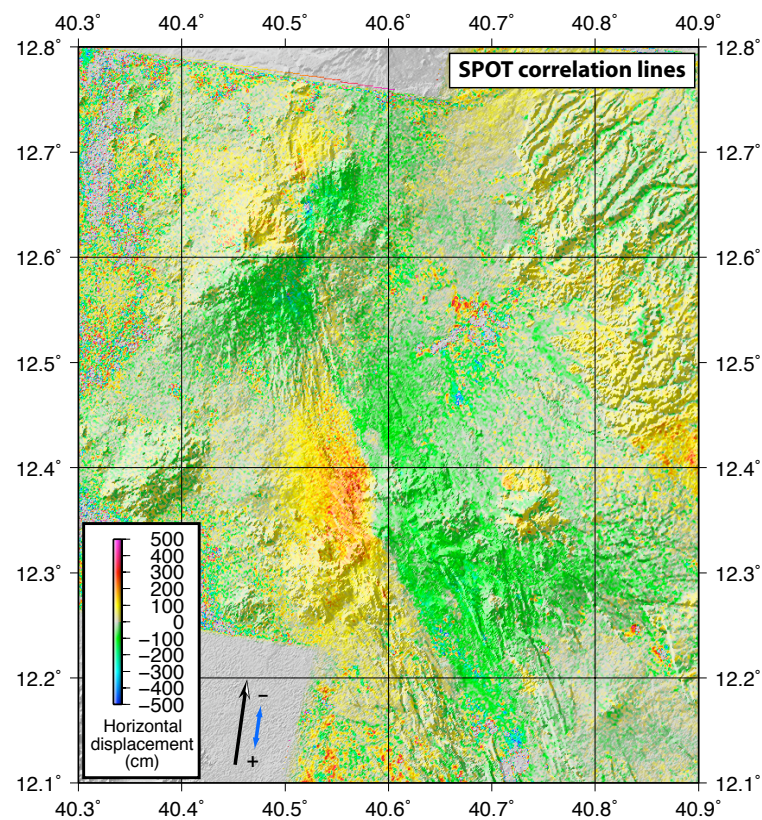
- Accuracy ~ 30 cm
- Measures horizontal displacements

⇒ Constrains horizontal displacements

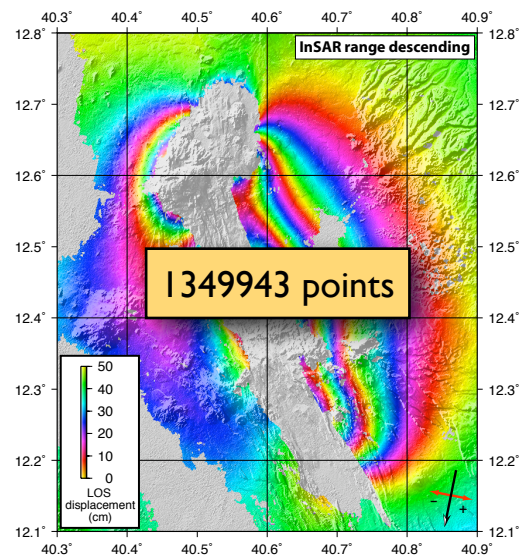
SPOT correlation data



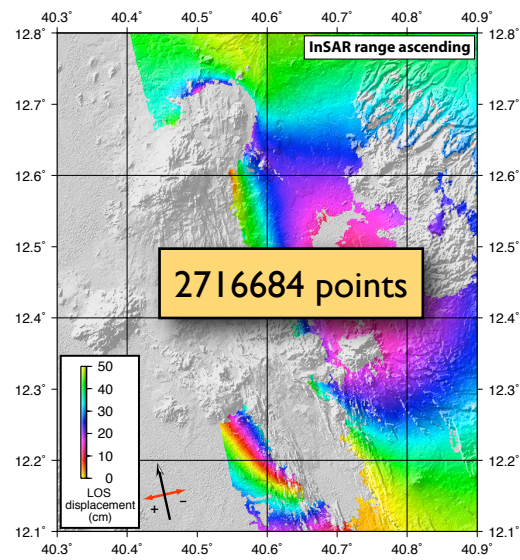
⇒ Constrains near-fault offsets



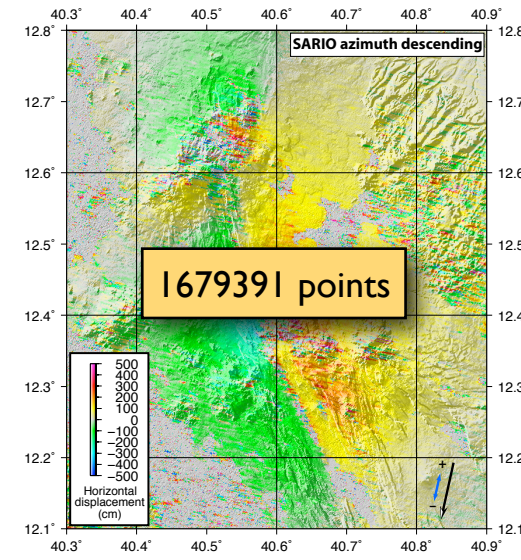
Data set overview



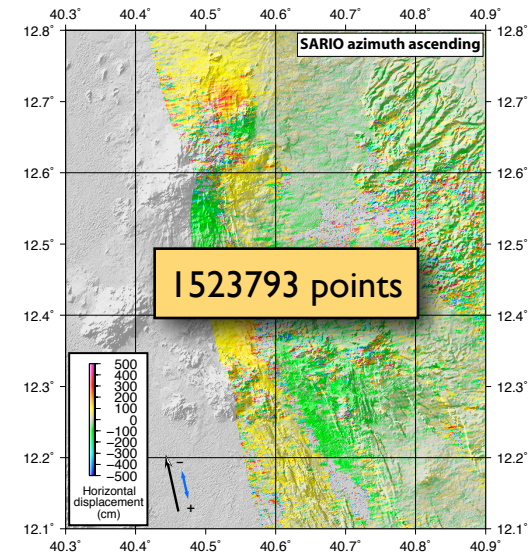
$\sigma \sim 0.3\text{cm}$



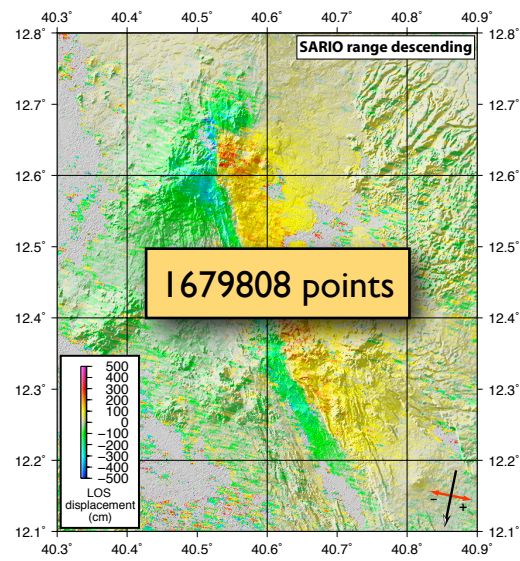
$\sigma \sim 0.3\text{cm}$



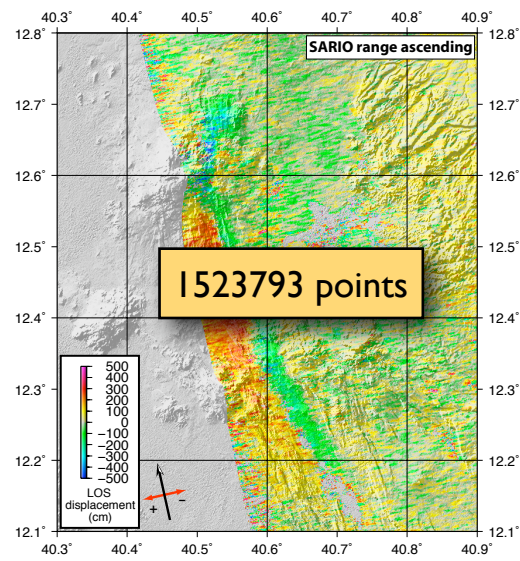
$\sigma \sim 30\text{cm}$



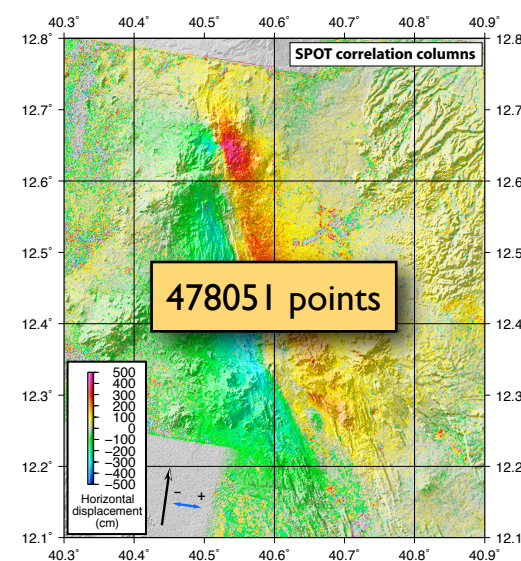
$\sigma \sim 30\text{cm}$



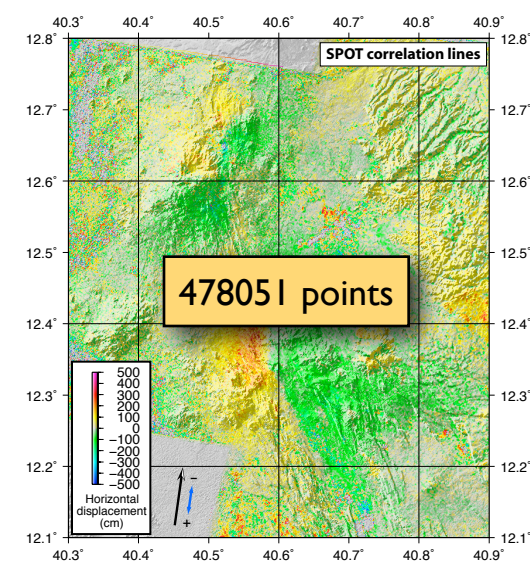
$\sigma \sim 50\text{cm}$



$\sigma \sim 50\text{cm}$



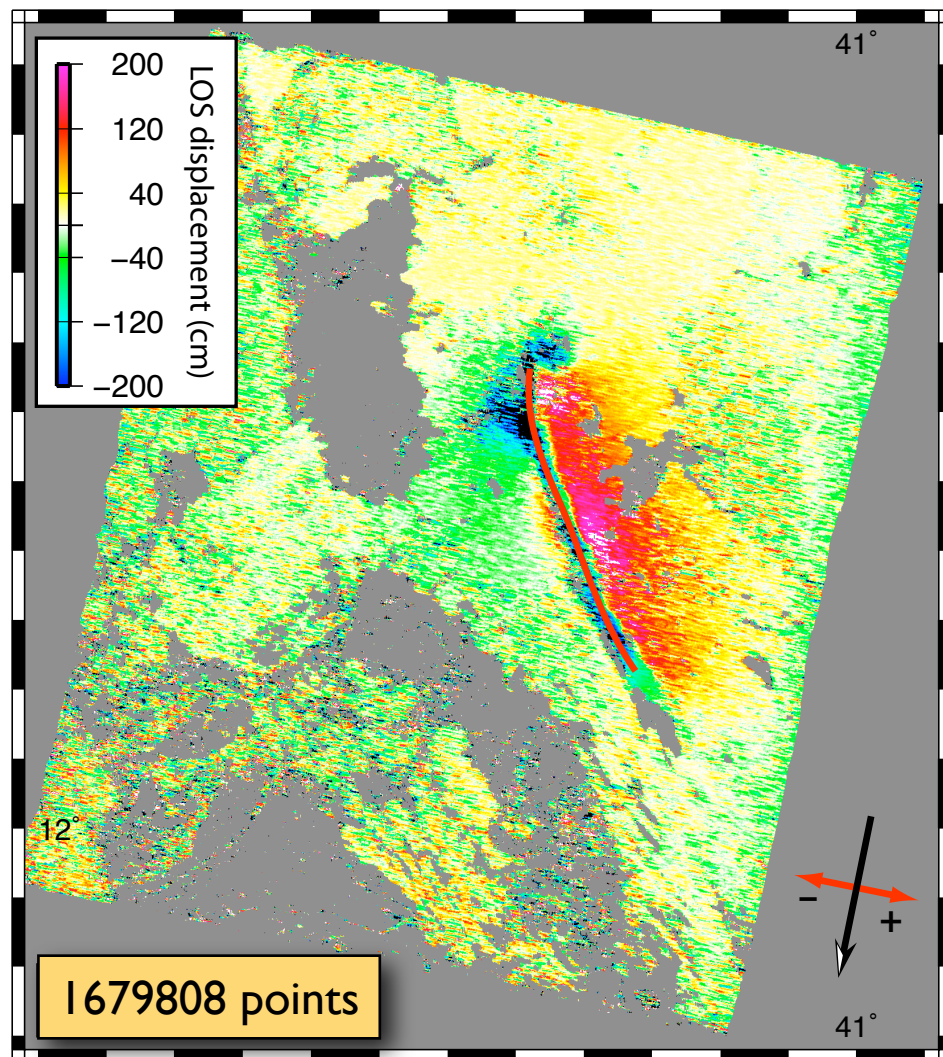
$\sigma \sim 10\text{cm HF}$
 $\sigma \sim 100\text{cm LF}$



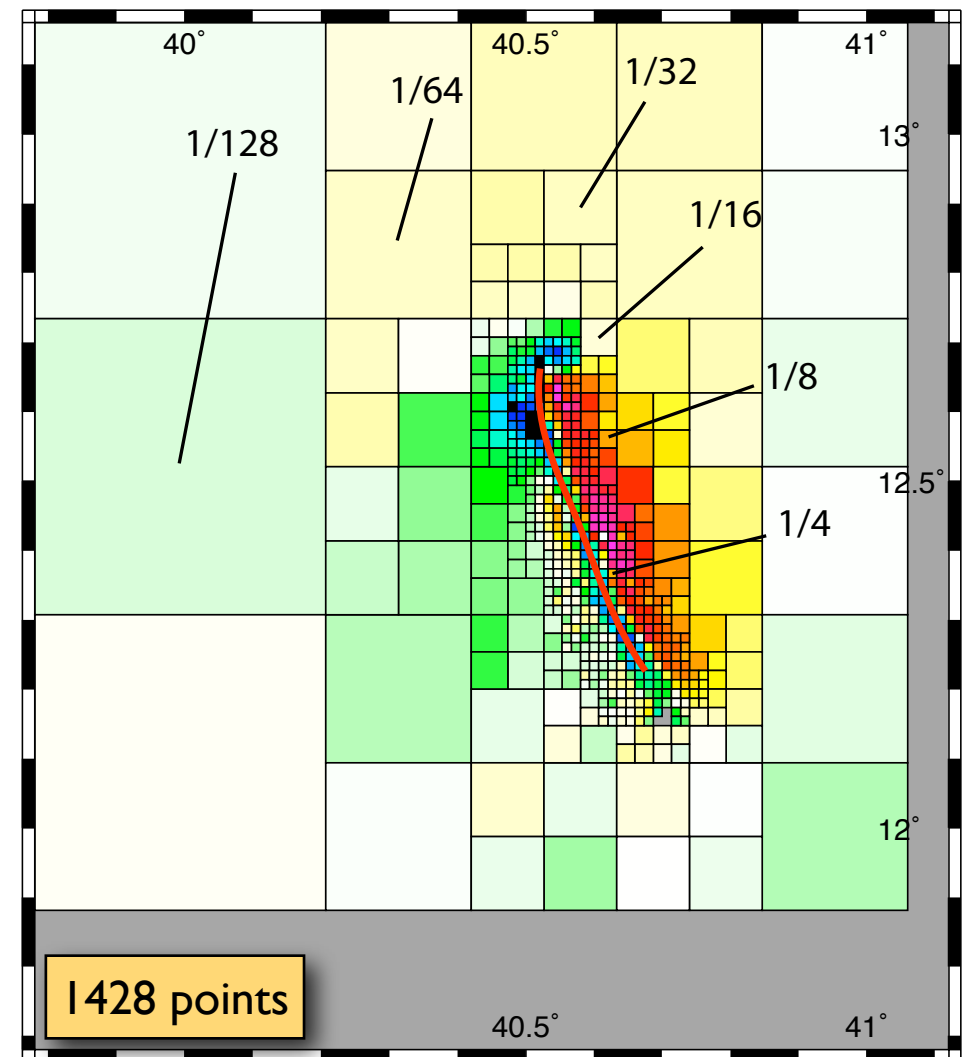
$\sigma \sim 10\text{cm HF}$
 $\sigma \sim 100\text{cm LF}$

⇒ Over 10 million points!

Data resampling



quadtree
resampling



- Measured displacements are averaged over a few pixels
- The size of the averaging area is a function of the distance to the assumed dike
- Sampling density increases when approaching the rift zone
- The relative sampling density between the various data sets is always constant

⇒ Less than 10000 points

Strategy for inversion

Initial assumption

Observed surface displacements can be explained by the opening, closure or slip on dislocations.

elasticity ➡ Okada (1985)

- opening of a vertical dislocation = dike
- slip on a dipping dislocation = fault
- closure of a horizontal dislocation = sill

1. Constrain the geometry of the dike and sills

non-linear ➡ Tarantola & Valette (1982)

- crude discretisation of the dike
- far-field data only

2. Constrain the geometry of the faults

non-linear ➡ Tarantola & Valette (1982)

- crude discretisation of the dike and faults
- near and far-field data

3. Invert for opening/slip with the resulting geometry

linear ➡ least-square inversion

- fine discretisation of the faults
- near and far-field data

➡ **Final model**

Inversion #1

Geometry:

- 3 dike segments
- 2 sills

Inverted parameters (for the dikes):

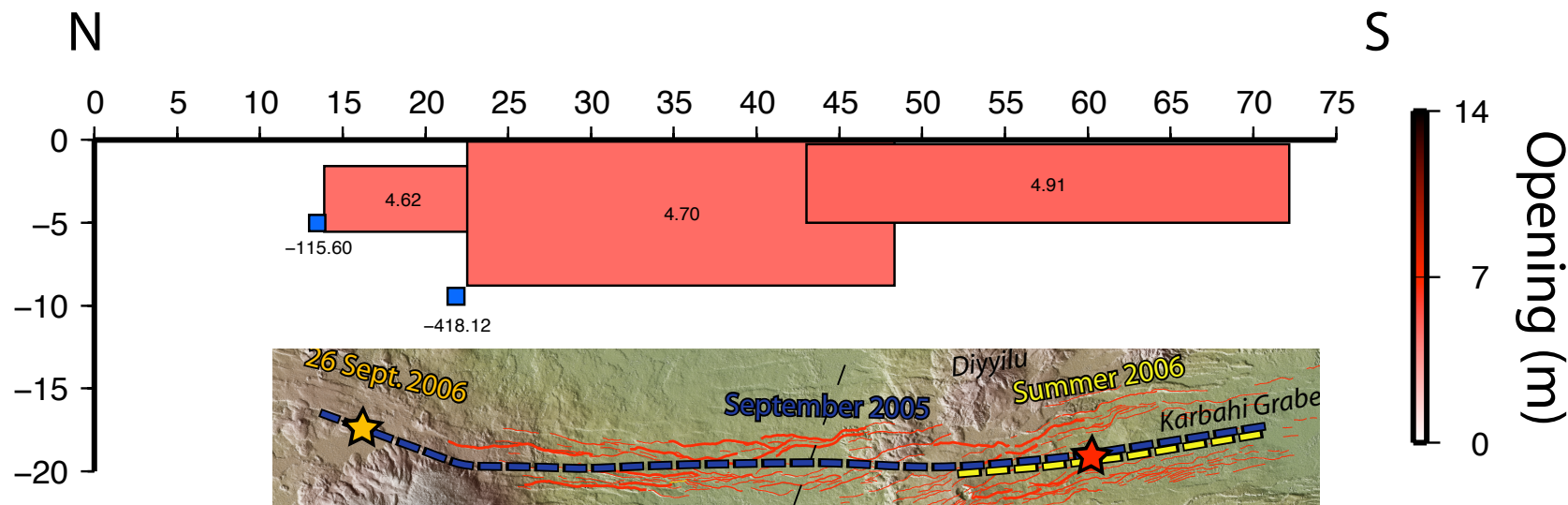
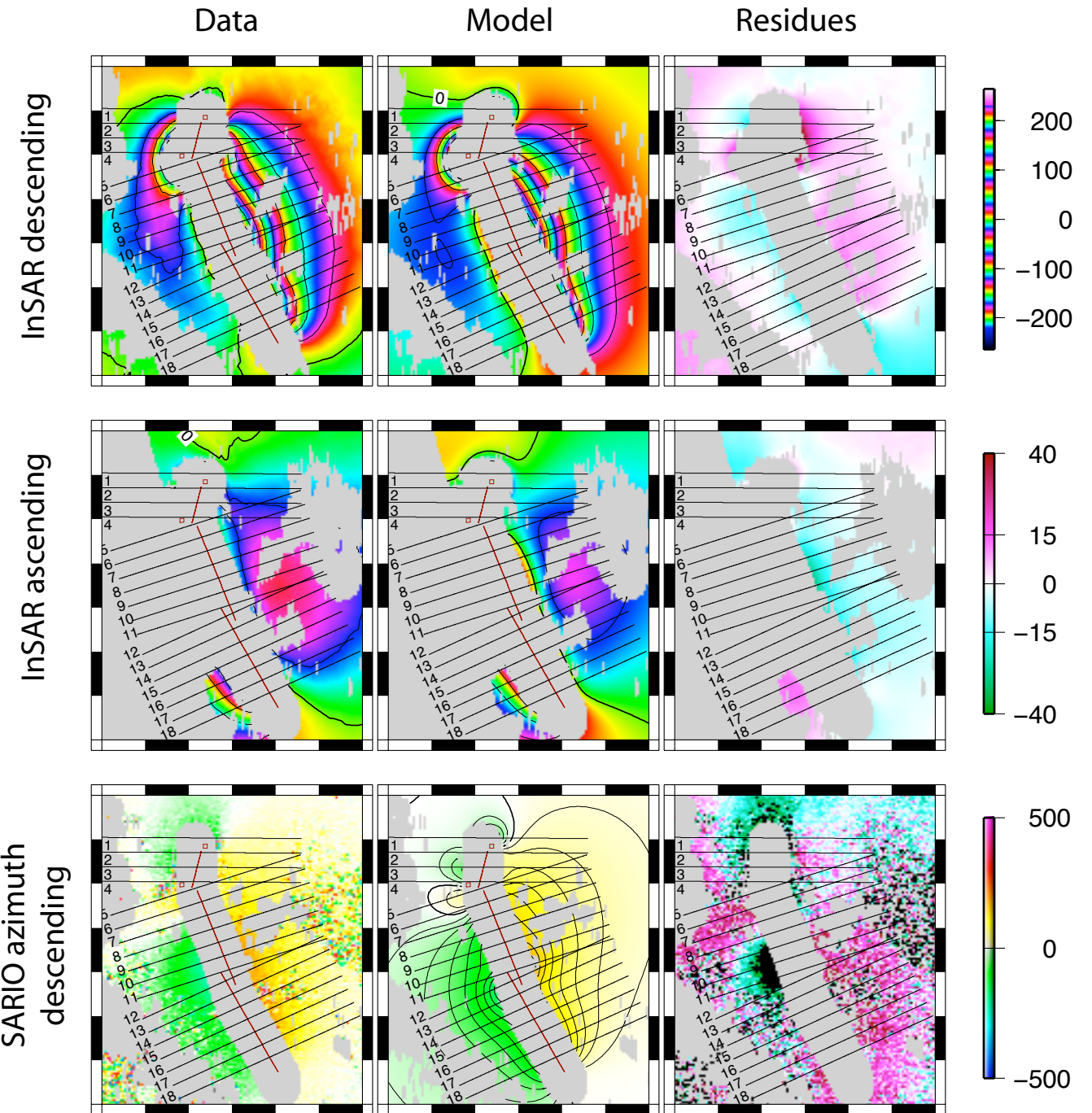
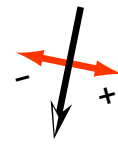
- opening
- position (longitude and latitude)
- width (bottom and top depths)
- length
- orientation (dip and strike)

Data sets used:

- InSAR descending
- InSAR ascending
- SARIO azimuth descending

► **31 parameters**

► **5936 data points**



⇒ Dike volume ~ 1.9 km³

⇒ Magmatic chamber deflation ~ 0.5 km³

Comparison with Summer 2006 intrusion events

Late September 2005

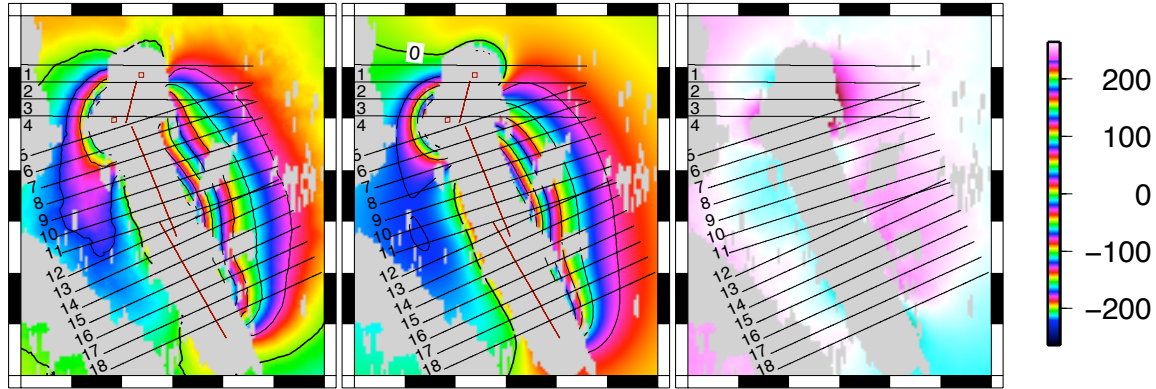
Npoints= 5936 RMS= 13.609689

Data

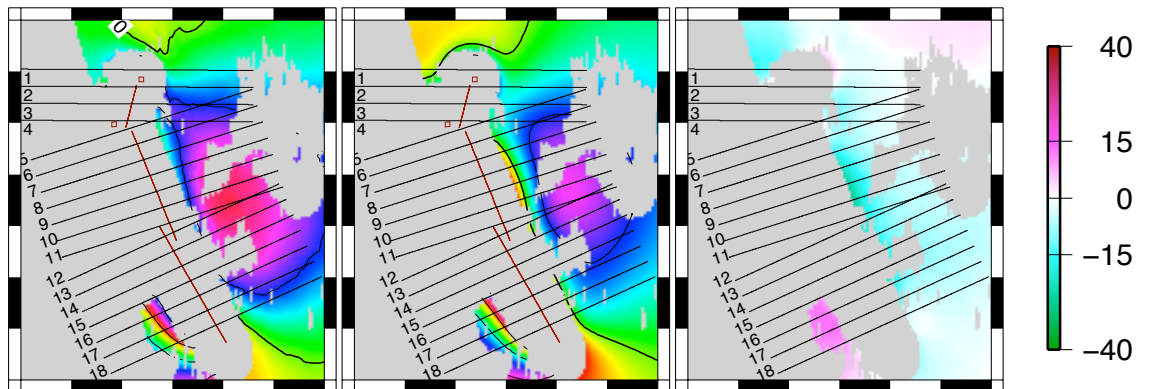
Model

Residues

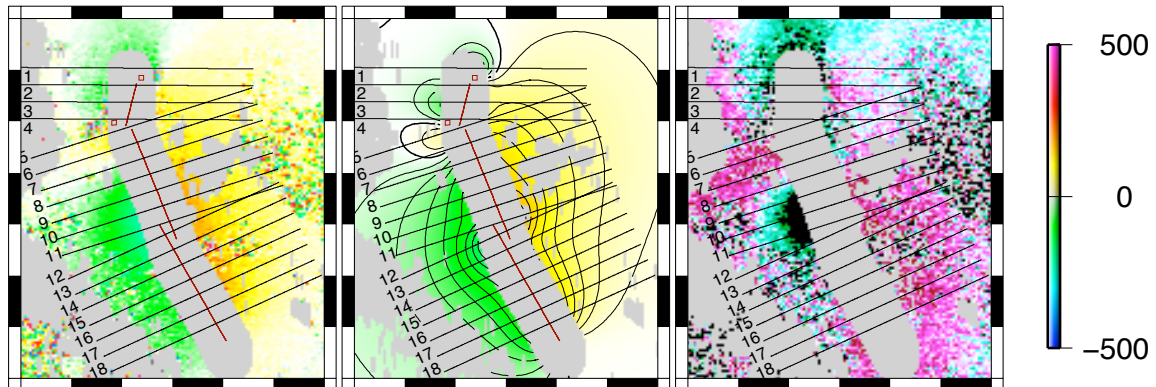
InSAR descending



InSAR ascending



SARIO azimuth
descending



June 17th 2006

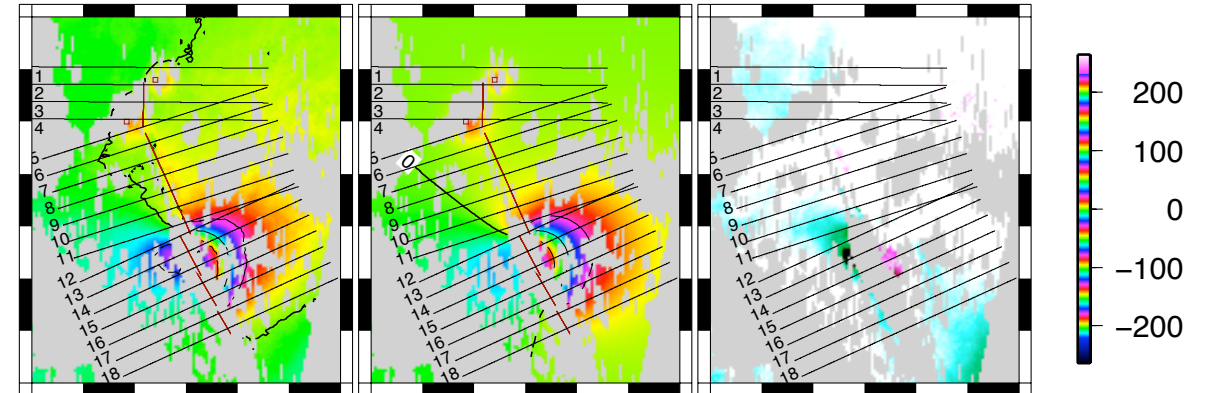
Npoints= 11250 RMS= 3.49

Data

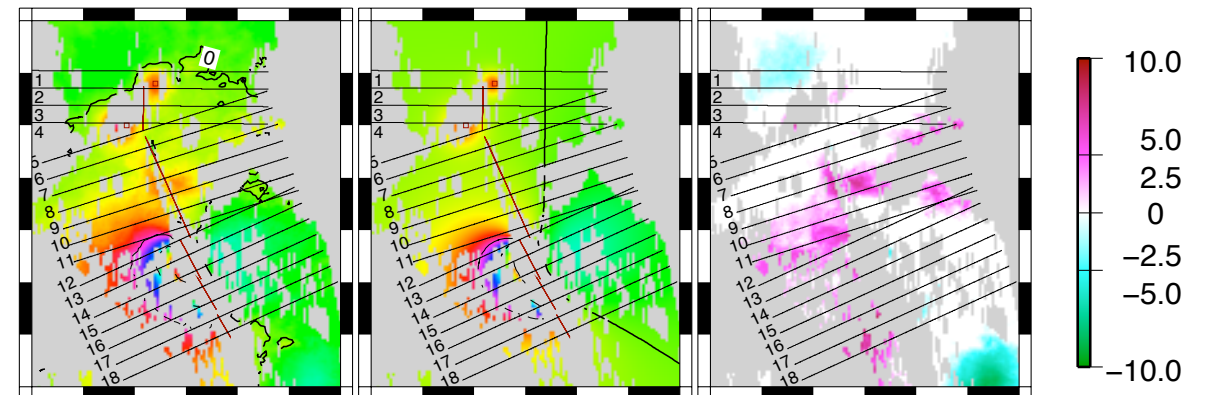
Model

Residues

InSAR descending



InSAR ascending

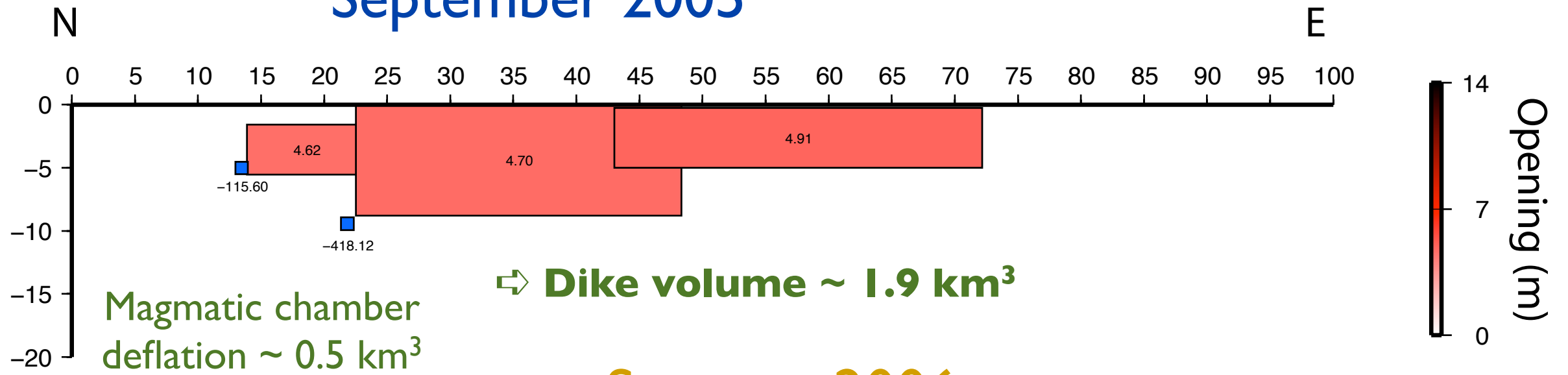


September 2005

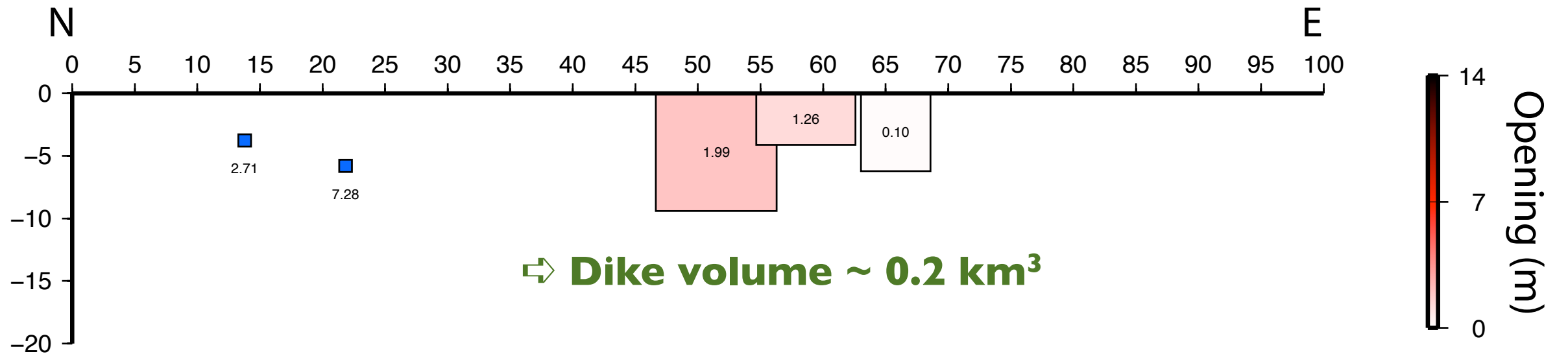
Summer 2006

Comparison with Summer 2006 intrusion events (2)

September 2005



Summer 2006



Inversion #2

Geometry:

- 8 dike segments
- 2 sills
- 30 faults (15 on each side)

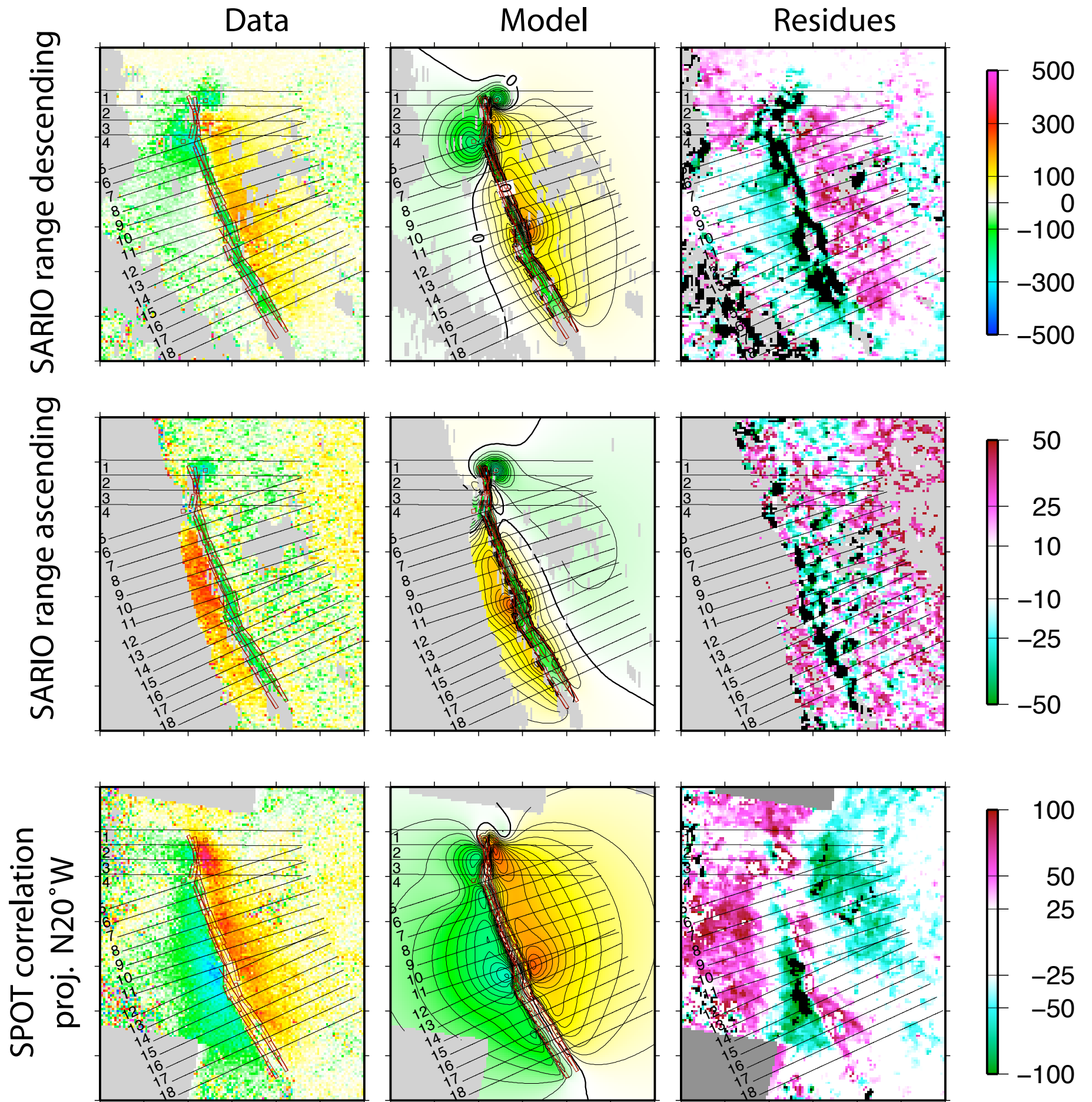
Inverted parameters (for the faults):

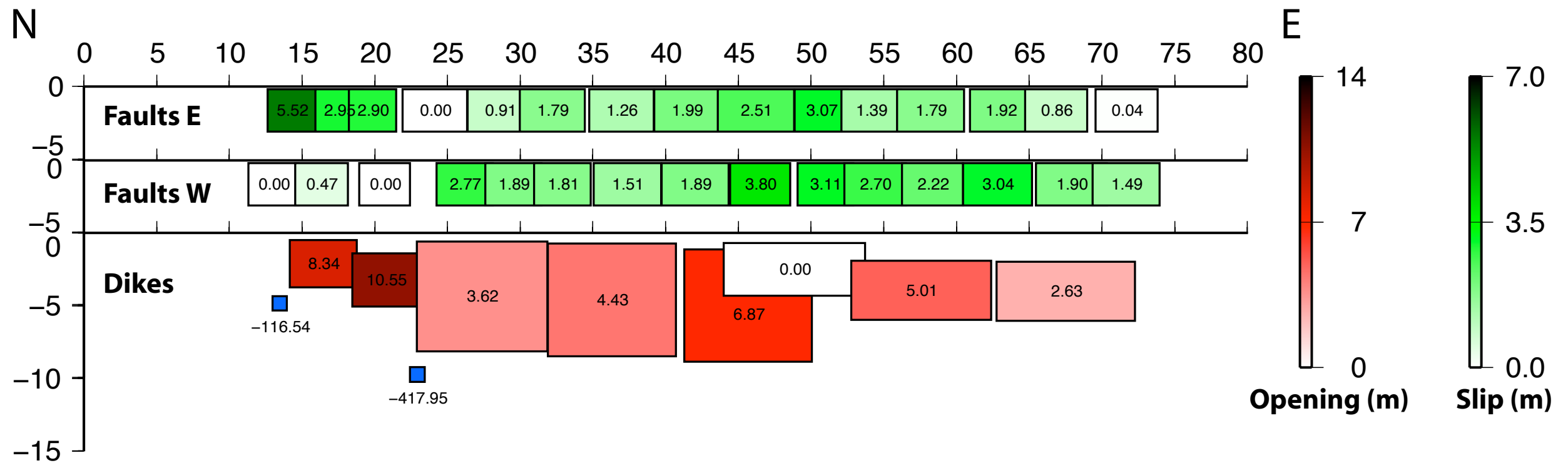
- slip
- position (longitude and latitude)

Data set used:

- InSAR, SARIO range and SARIO azimuth descending
- InSAR, SARIO range and SARIO azimuth ascending
- SPOT offsets

- ▶ **138 parameters**
- ▶ **7024 data points**





- ⇒ Greatest opening along the Dabbahu segment, but at shallow depth ⇒ smaller volume
- ⇒ Asymmetric slip along Dabba'hu segment
- ⇒ Opening is maximum at the junction between the northern segment and the southern segment

Inversion #3

Geometry:

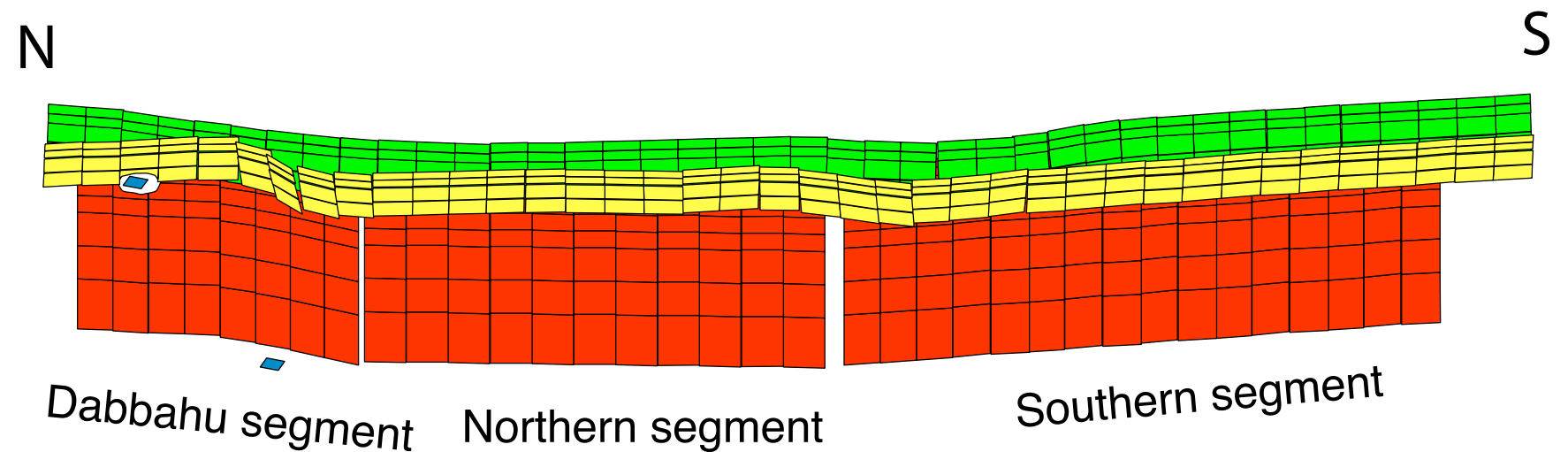
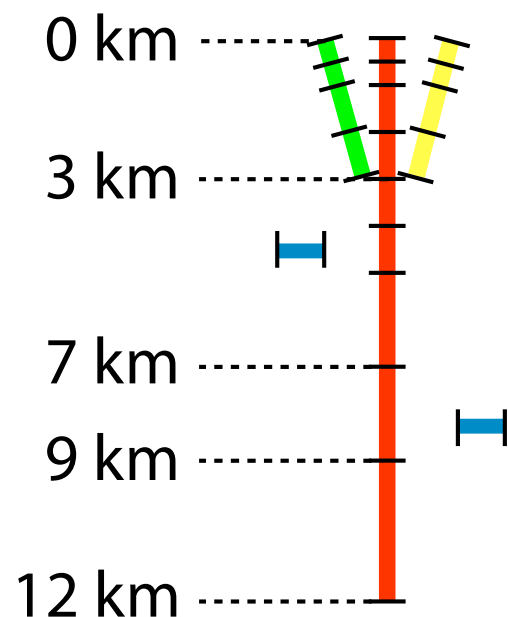
- 315 dike segments
- 2 sills
- 320 faults (160 on each side)

Data sets used:

- InSAR, SARIO range and SARIO azimuth descending
- InSAR, SARIO range and SARIO azimuth ascending
- SPOT offsets

► **957 parameters**

► **7024 data points**



Inverted parameters (for the faults):

- slip and opening

Inverted parameters (for the dikes):

- opening

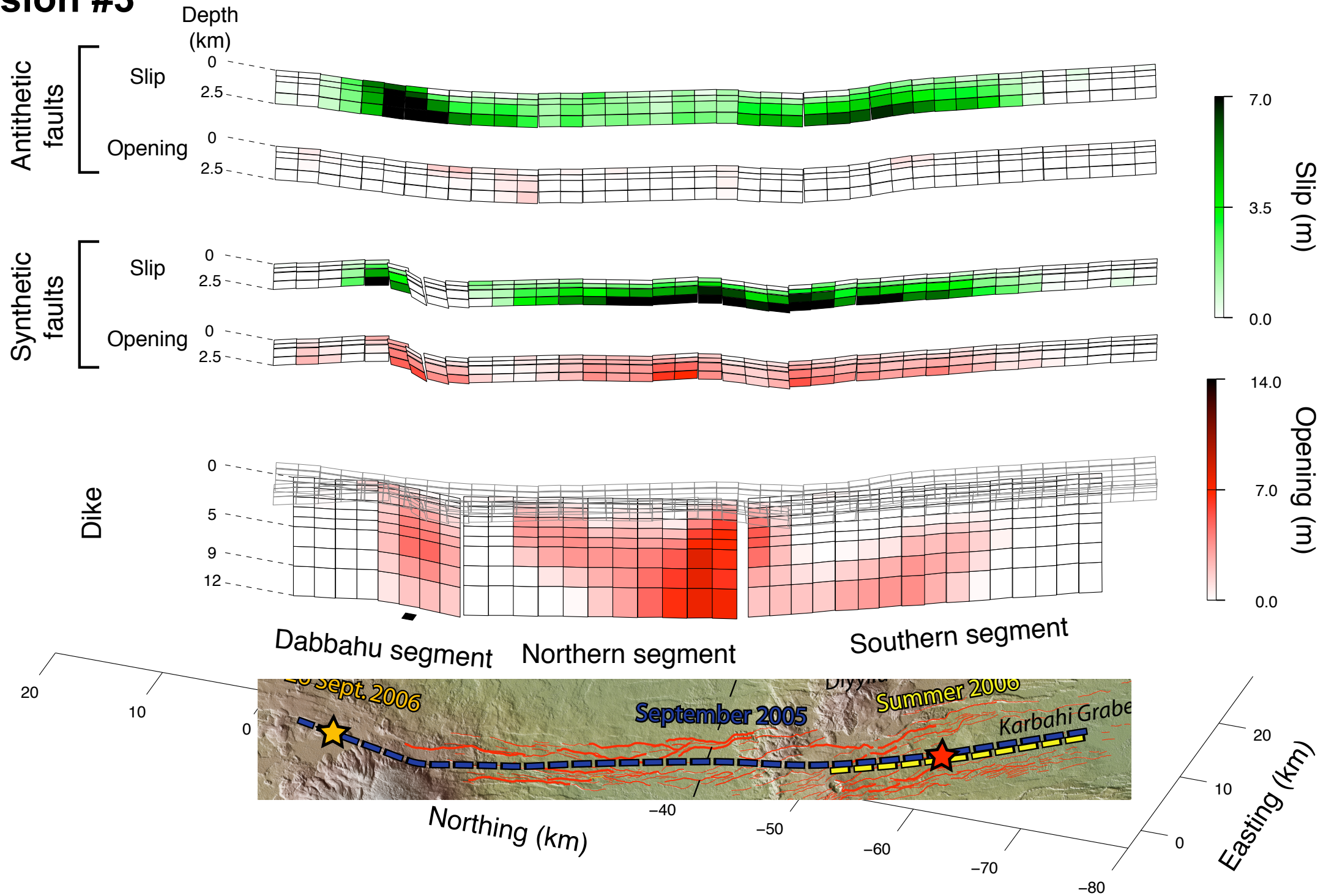
Inverted parameters (for the sills):

- closure

Additional constraints:

- non-negativity
- Laplacian smoothing (Menke, 1984)

Inversion #3

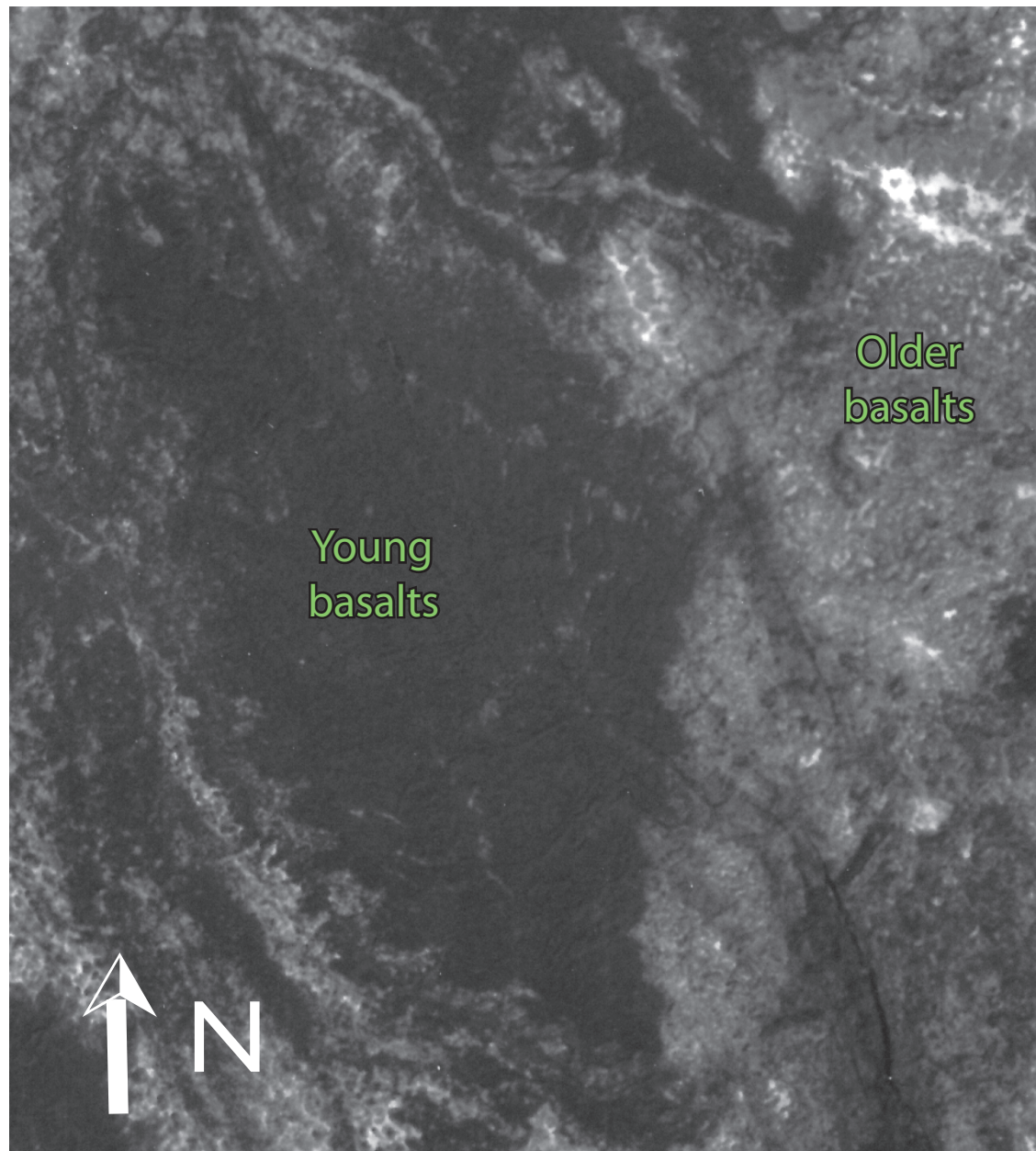


⇒ Asymmetric slip along the Dabbahu segment

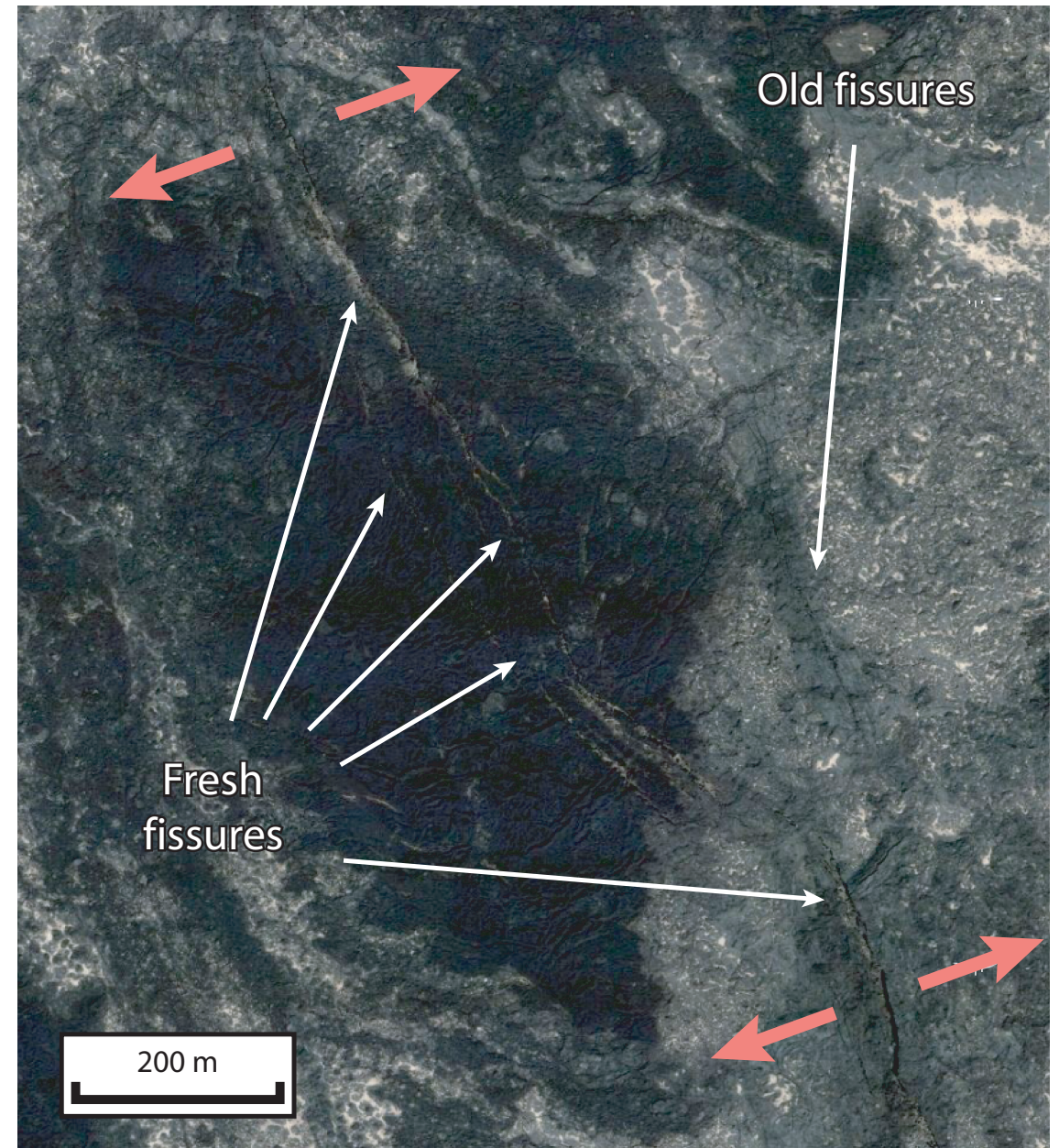
⇒ Opening is deepest at the junction between northern and southern segments

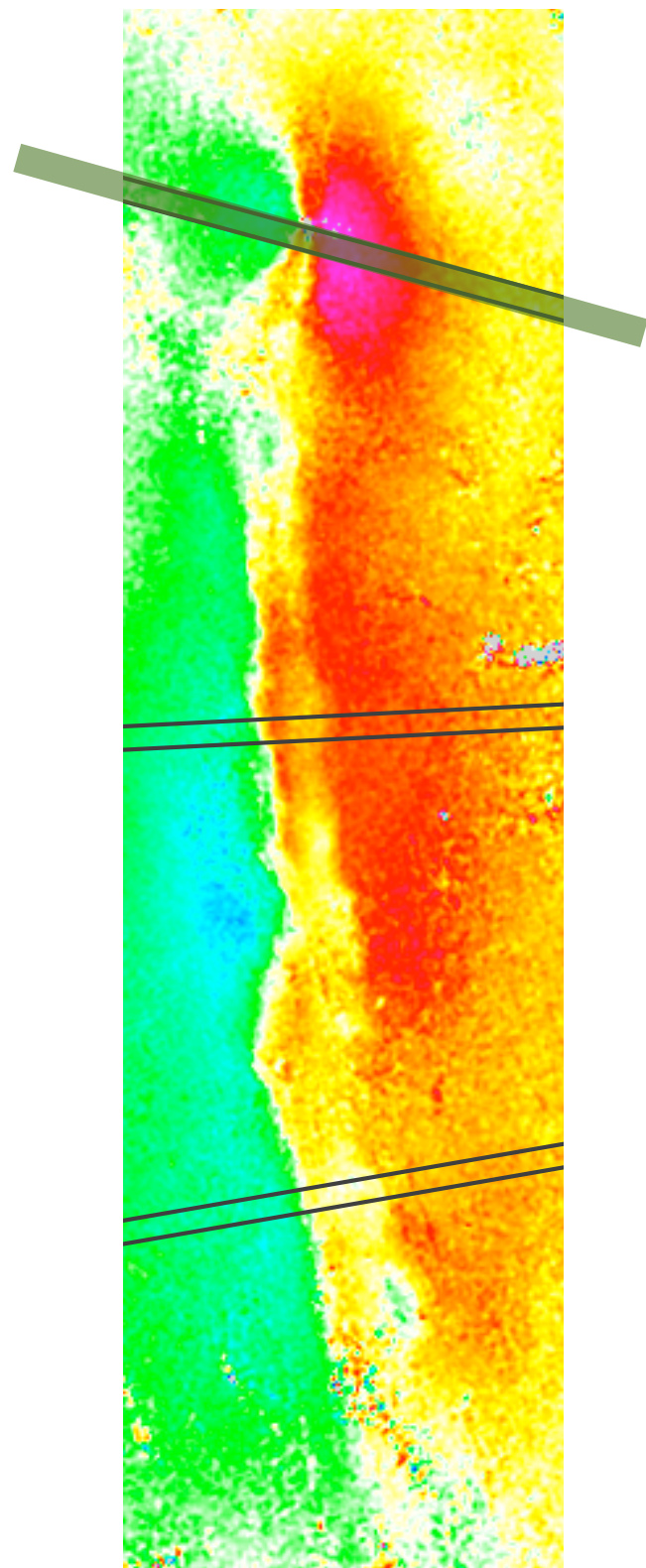
⇒ Significant opening on, or close to, synthetic faults (eastward dipping)

Aerial photography
1994

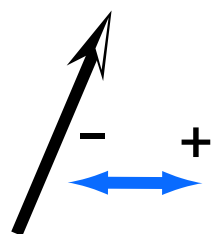
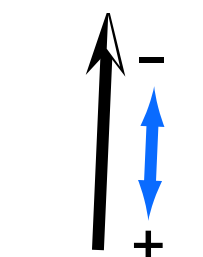
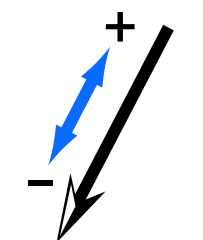
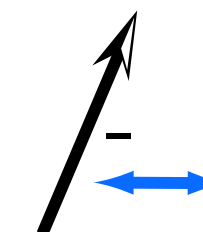
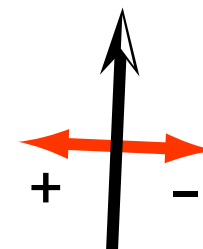
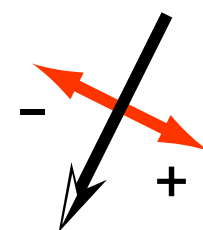
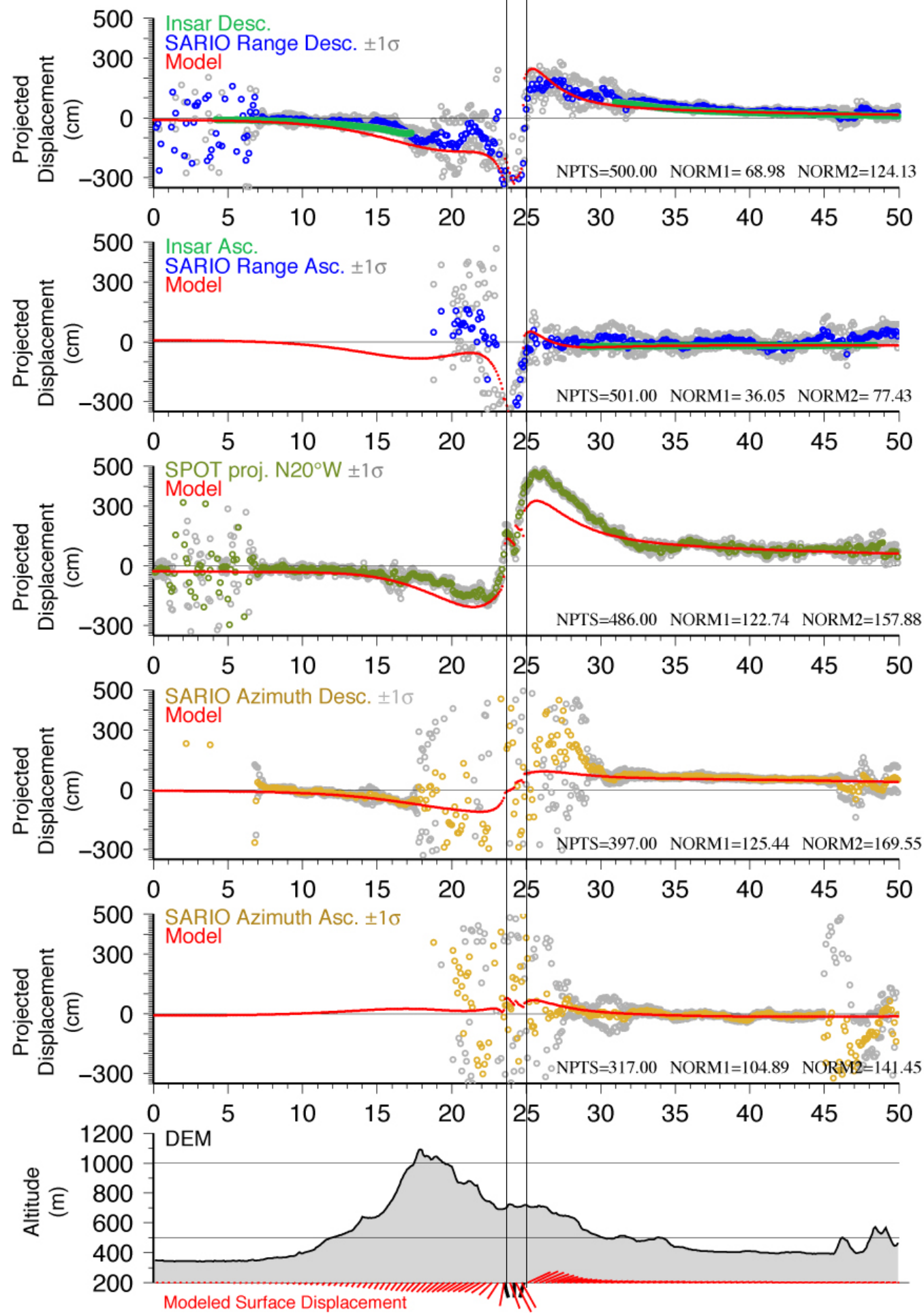


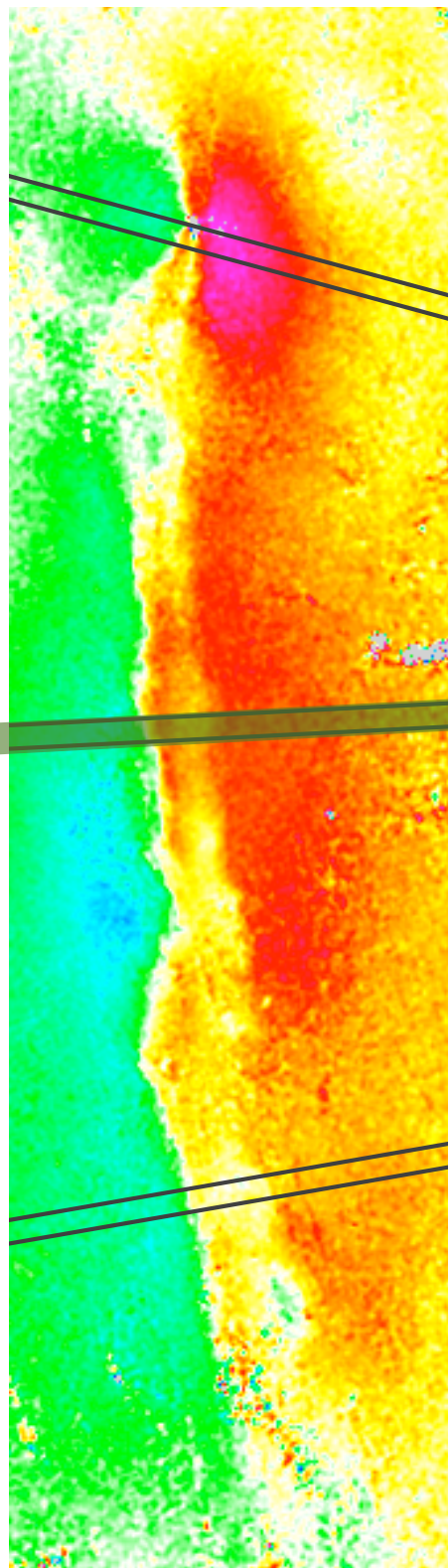
Quickbird image
2006



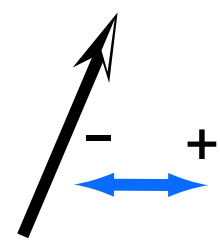
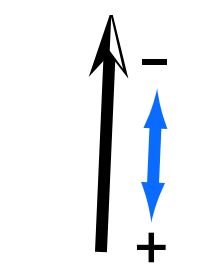
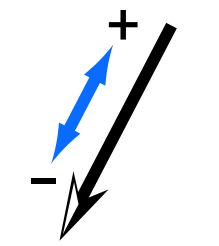
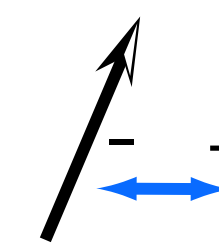
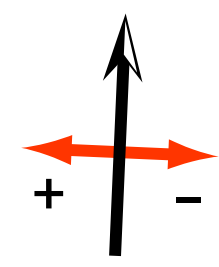
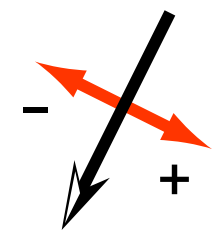
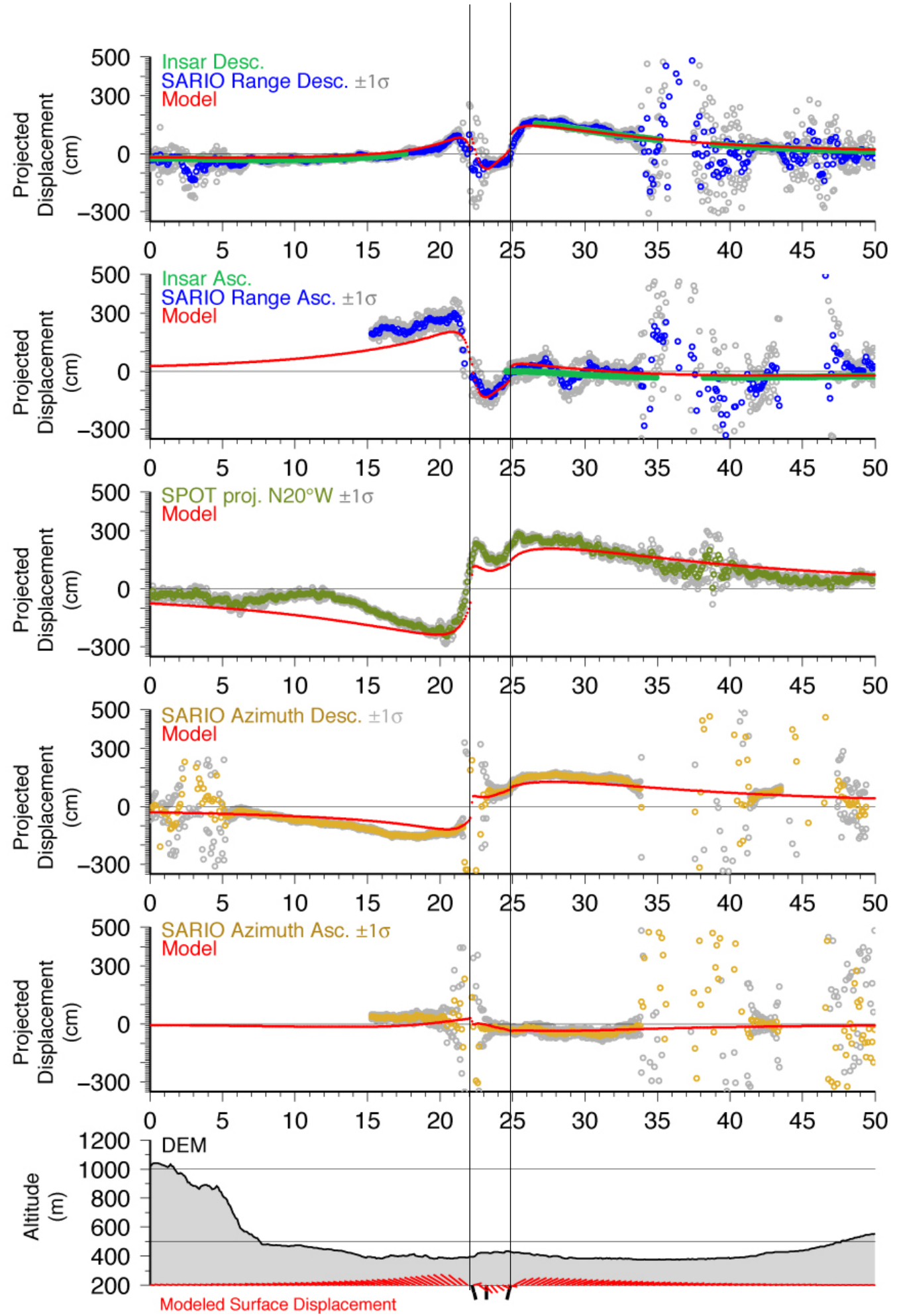


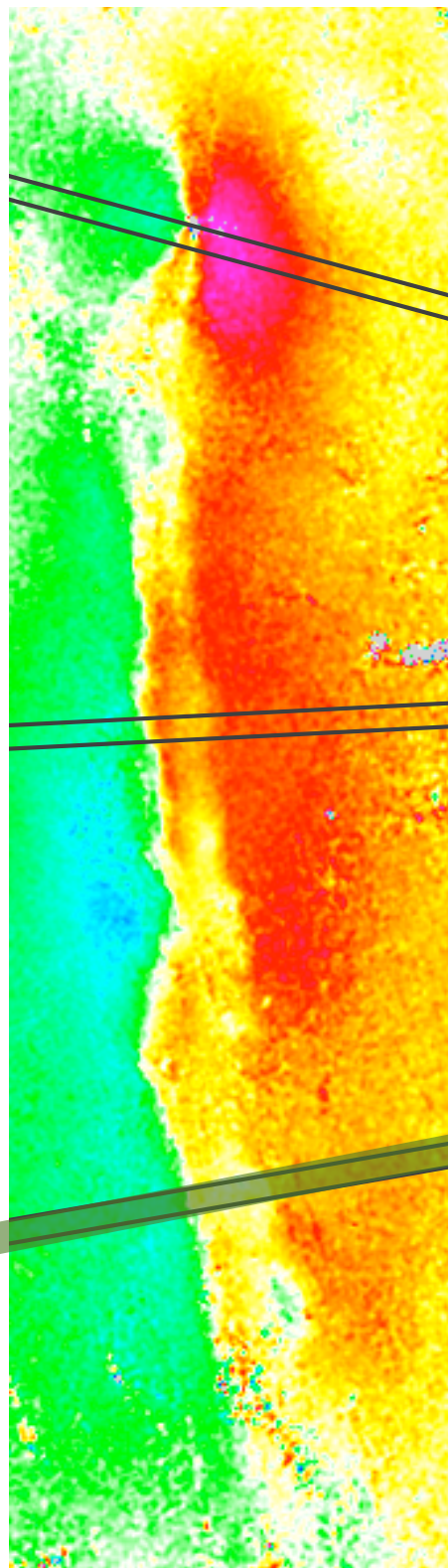
a



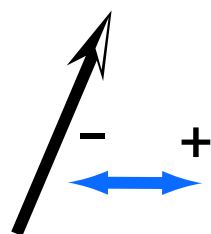
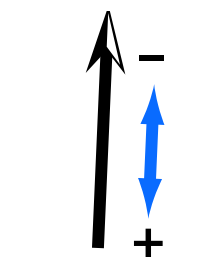
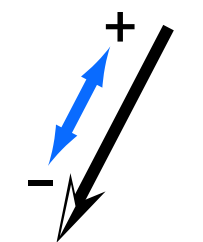
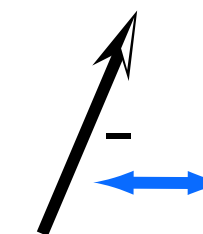
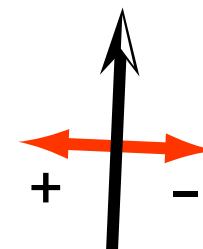
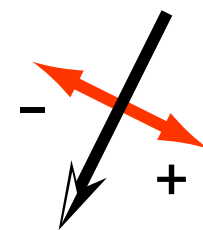
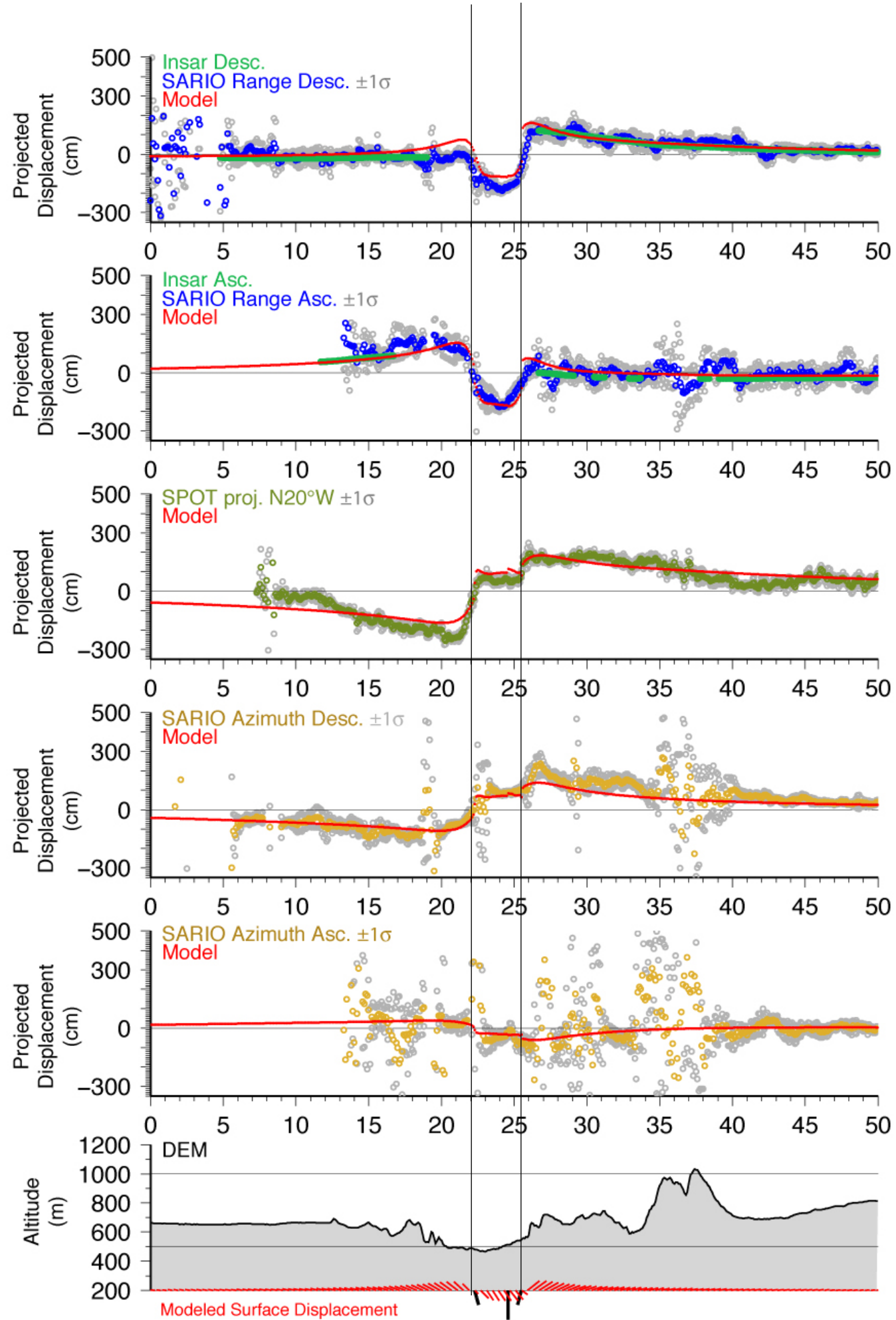


b

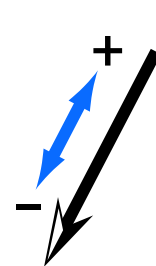
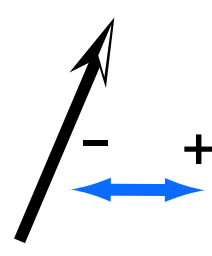
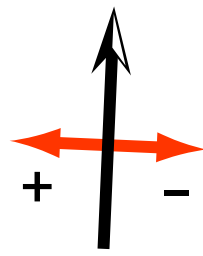
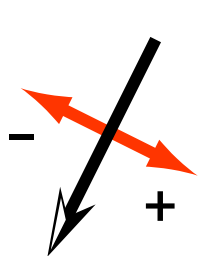
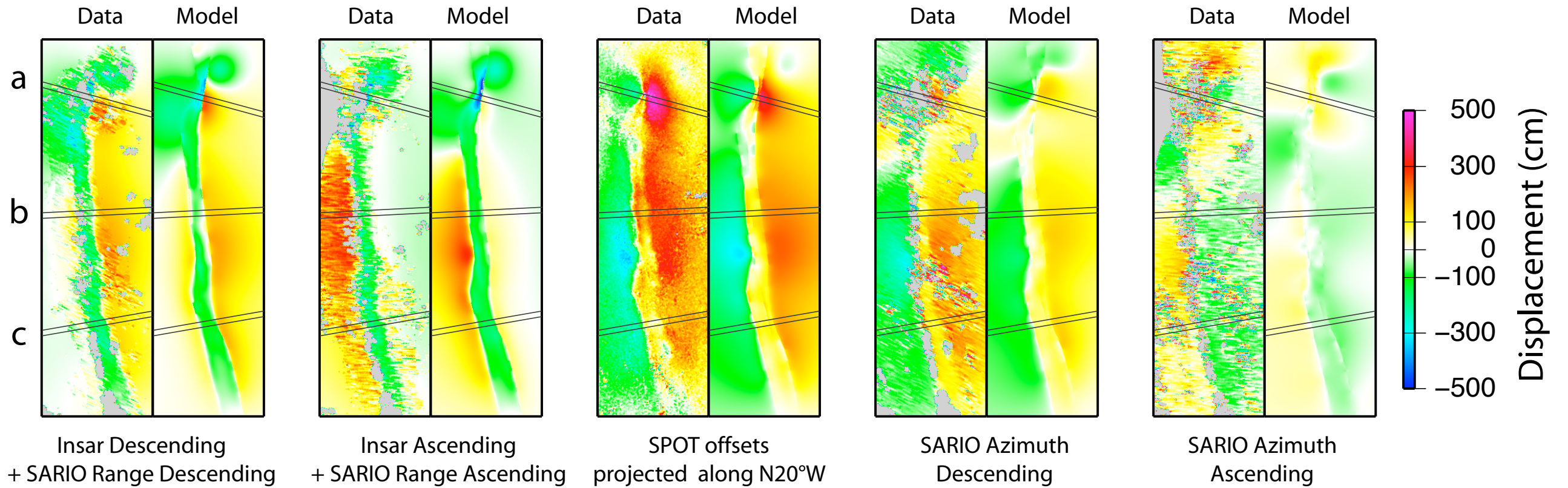




C



Inversion #3



⇒ Explains most of the data set

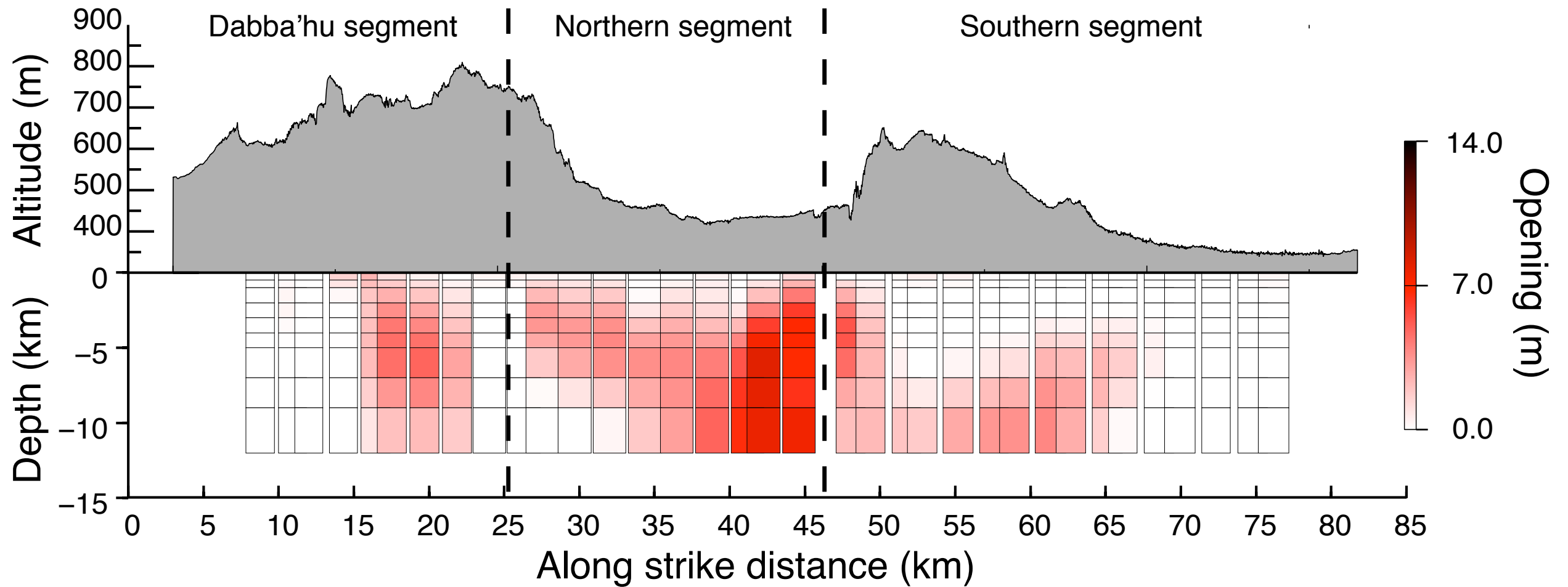
⇒ Robust result

but ... slight underestimation of horizontal displacements
and ... several small scale problems

Summary & possible conclusions

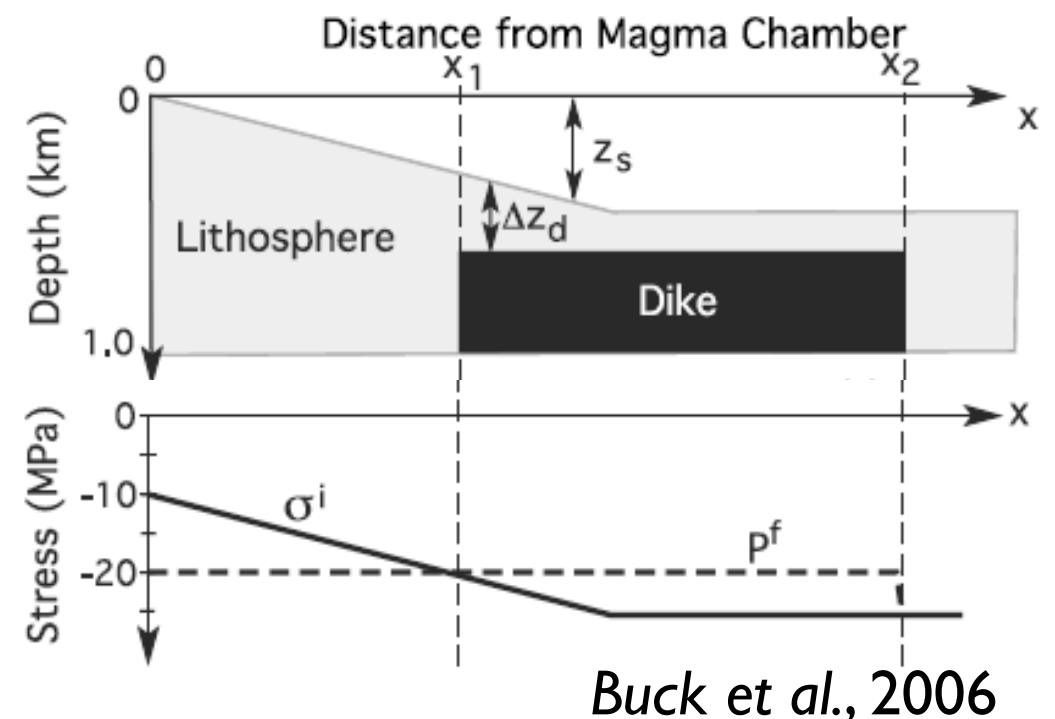
- ⇒ Dike volume $\sim 1.9 \text{ km}^3$
 - ⇒ Magmatic chamber deflation $\sim 0.5 \text{ km}^3$
- ⇒ Shallow opening west of Dabba'hu, with asymmetric slip
- ⇒ Largest and deepest opening at Ado'Ale
- ⇒ Northern segment: opening and slip at shallow depth on or close to synthetic (eastward dipping) faults ; no opening on antithetic faults, with less slip
- ⇒ Southern segment: more symmetrical behavior along the southern segment
- ⇒ Requires another source for at least 2/3 of the basaltic magma
- ⇒ Importance of segmentation
- ⇒ Shallow silisic dike originating from the Gabho magmatic chamber?
- ⇒ Locus of basaltic magma input?
- ⇒ Magma assisted faulting?
 - ⇒ Block rotations?
- ⇒ Displacements observed at the surface are conditioned by the location of the dike with respect to the rift axis

Along strike topography VS opening

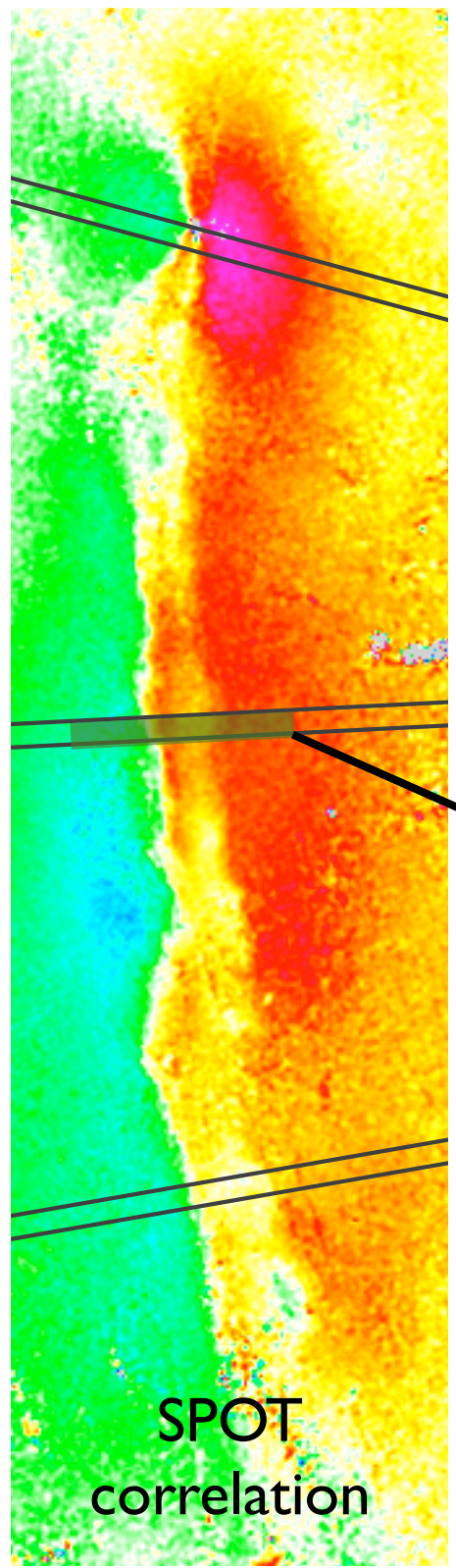


High topography = stress barrier for the dike?

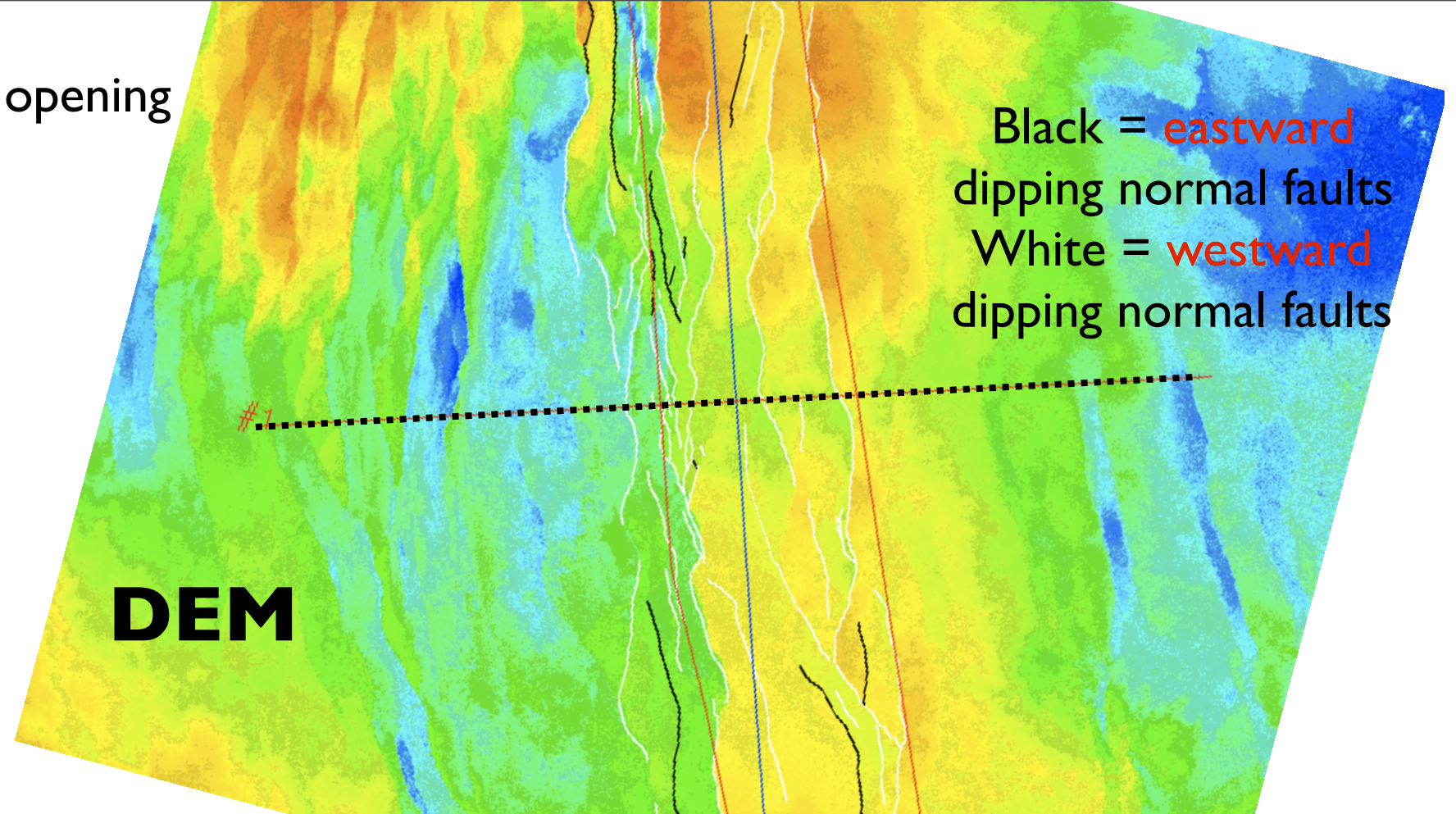
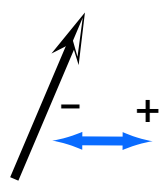
⇒ If so, when and how is extension accommodated in areas where opening is “bottlenecked”?



Rift perpendicular topography VS opening

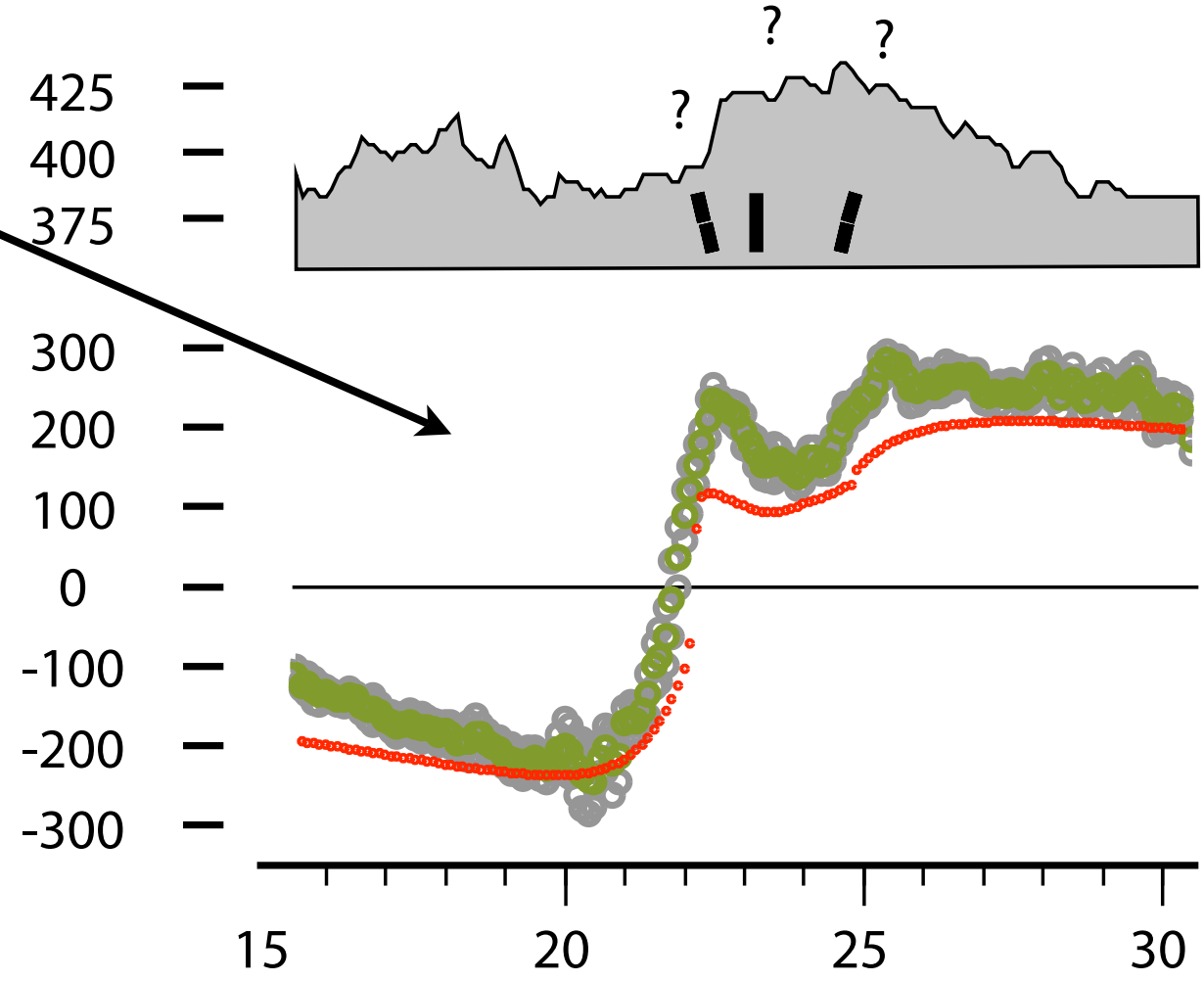


SPOT correlation



Black = eastward dipping normal faults
White = westward dipping normal faults

DEM



425
400
375

300
200
100
0
-100
-200
-300

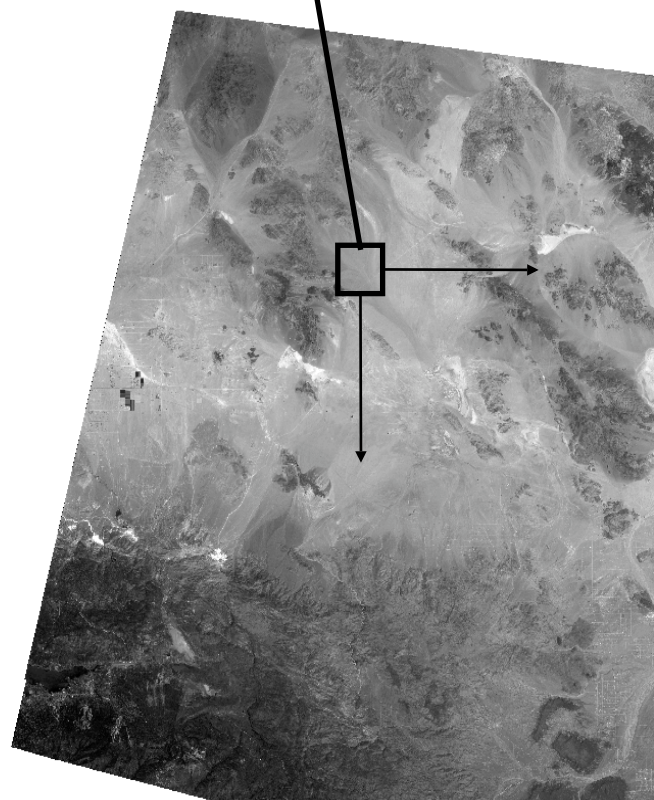
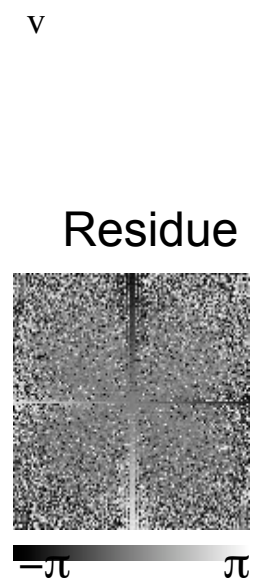
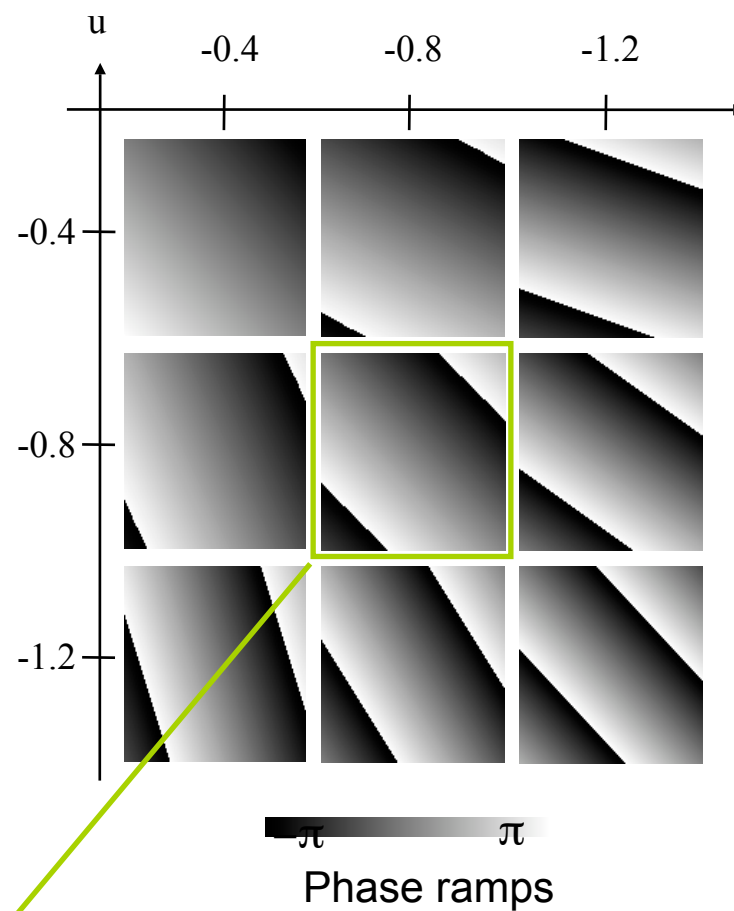
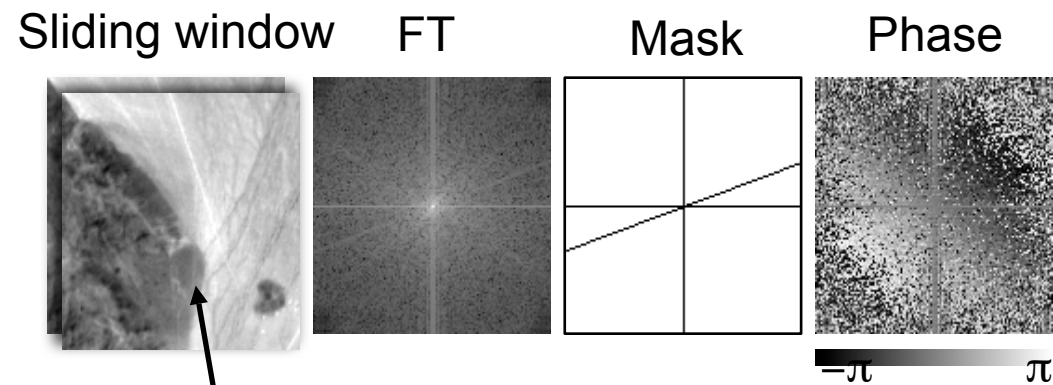
15 20 25 30

Thank you for your attention!

Sub-pixel correlation of optical images: principle

$$I_2(c, l) = I_1(c + u_0, l + v_0)$$

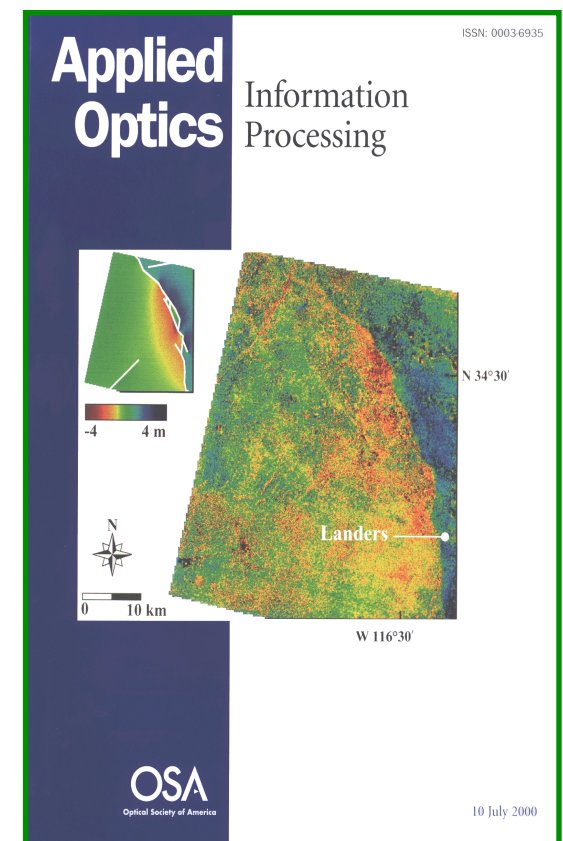
$$TF(I_2) = TF(I_1) \cdot e^{2i\pi(w_c u_0 + w_l v_0)}$$



Best Model

$$(u, v) = \underset{(u_o, v_o)}{\text{Arg}} \left(\max_{\text{mask}} \left| \sum \exp[i \cdot \Phi] \exp[-2\pi i \cdot (w_c \cdot u_o + w_l \cdot v_o)] \right| \right)$$

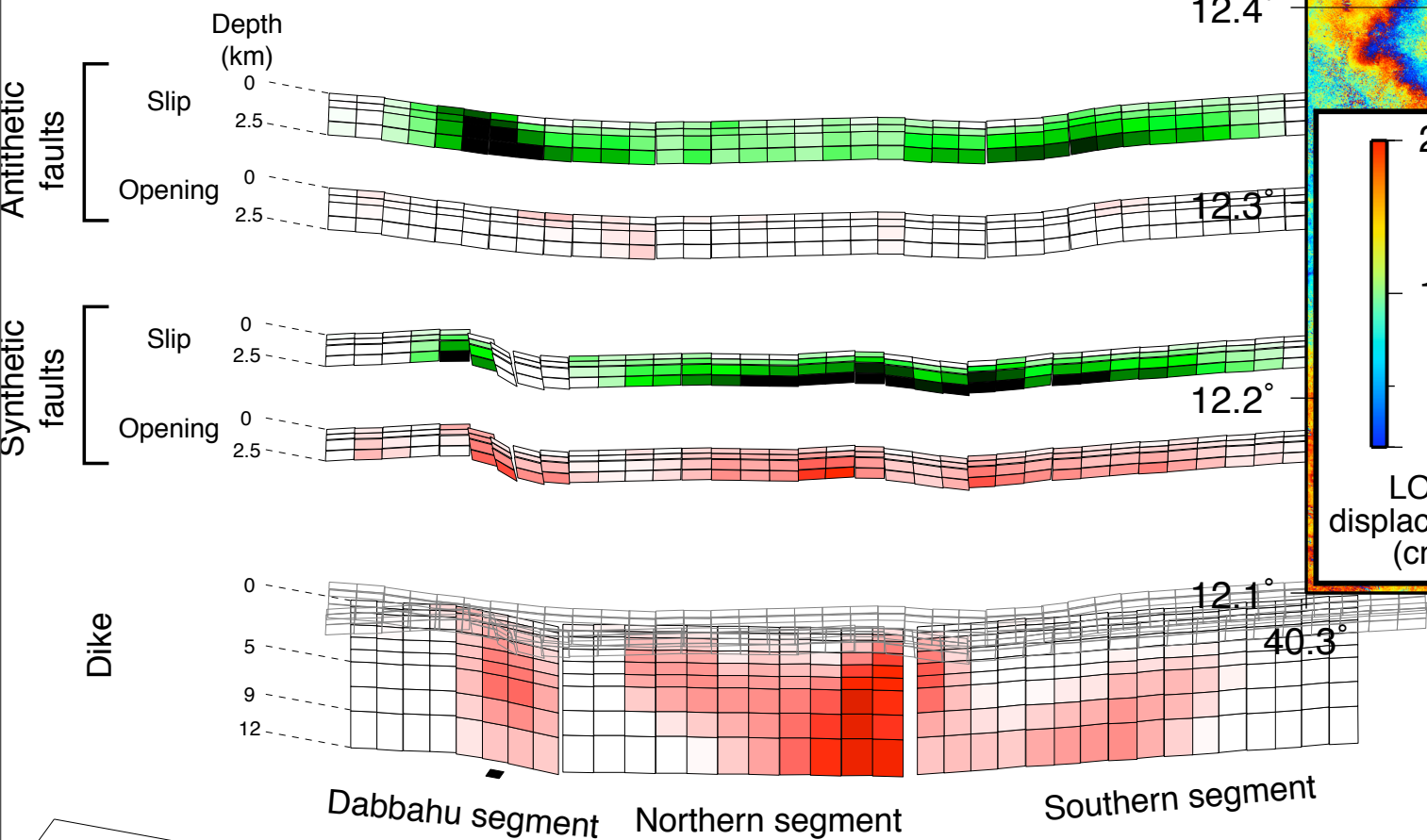
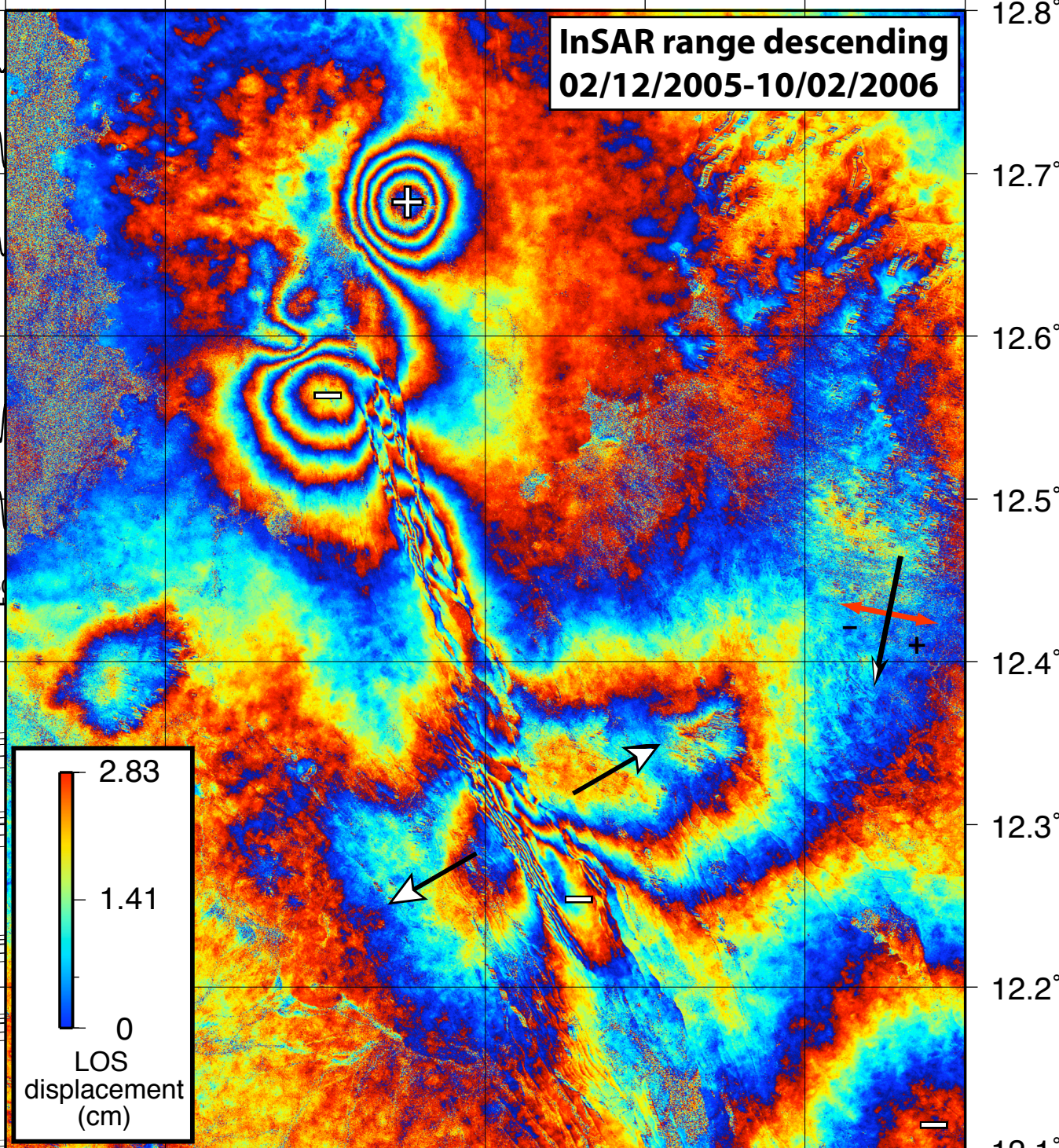
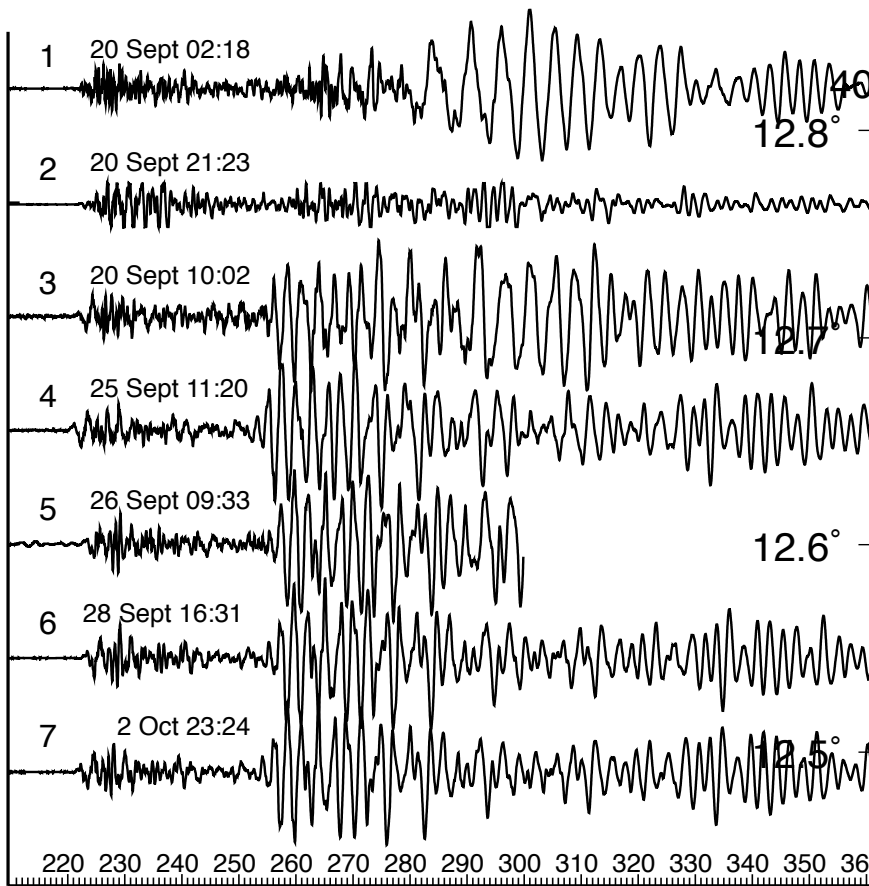
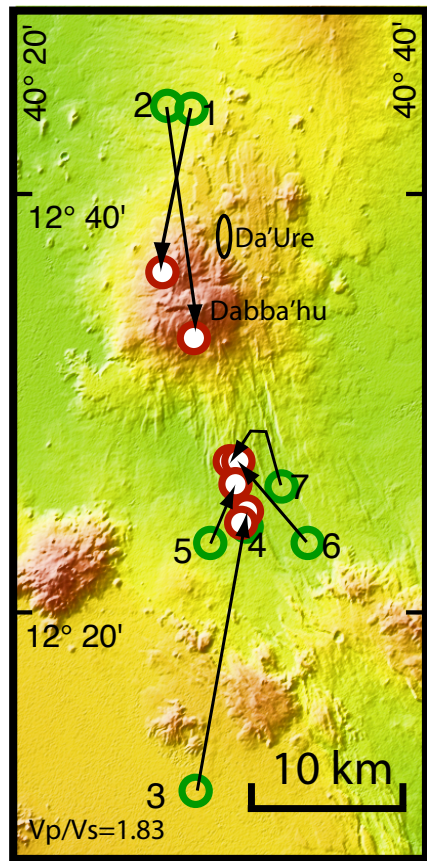
$$\text{snr} = \left| \sum_{\text{mask}} \exp[i \cdot \Phi] \exp[-2\pi i \cdot (w_c \cdot u + w_l \cdot v)] \right|$$



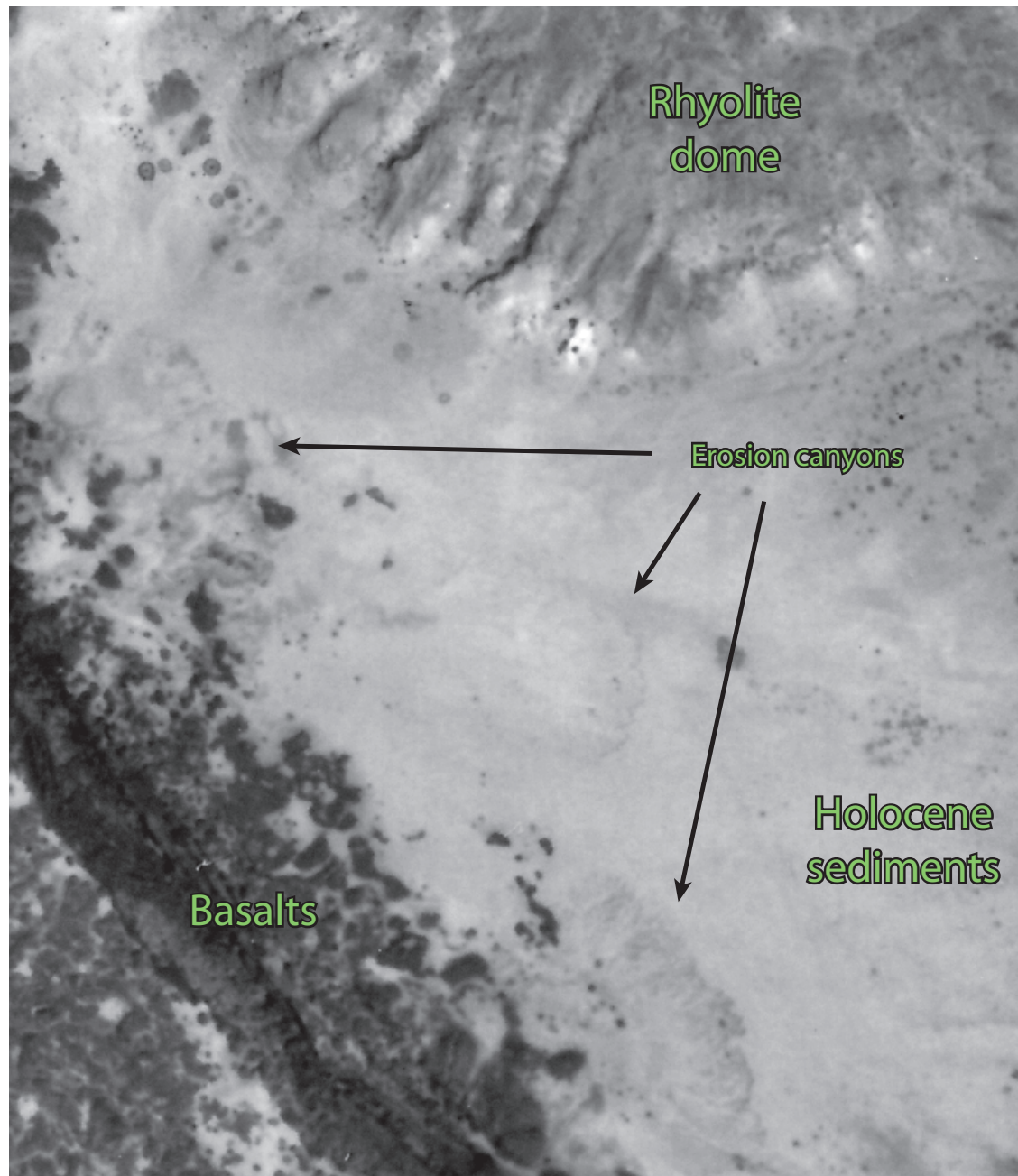
Landers

Michel, Van Puymbroeck, Binet

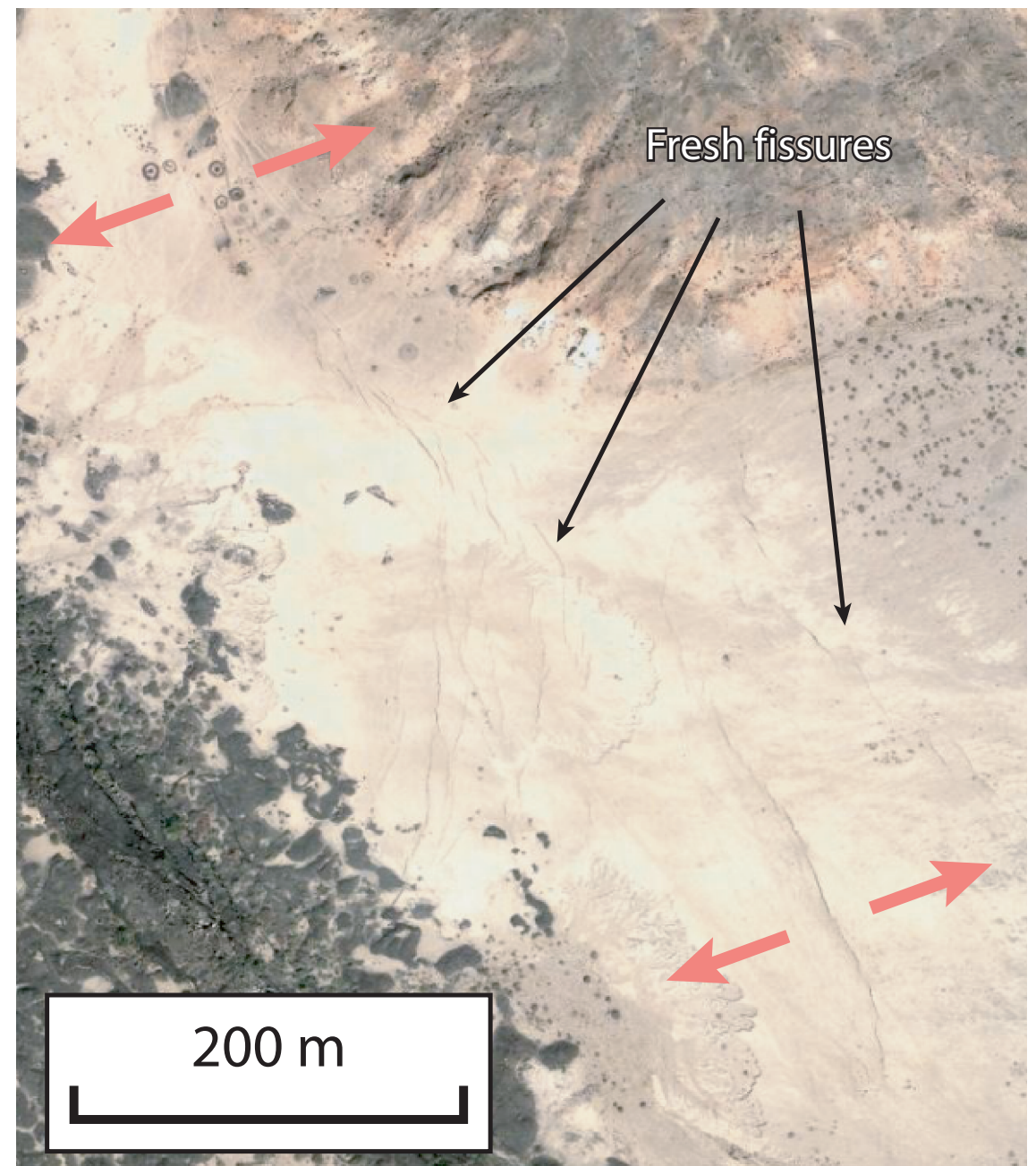
Segmentation



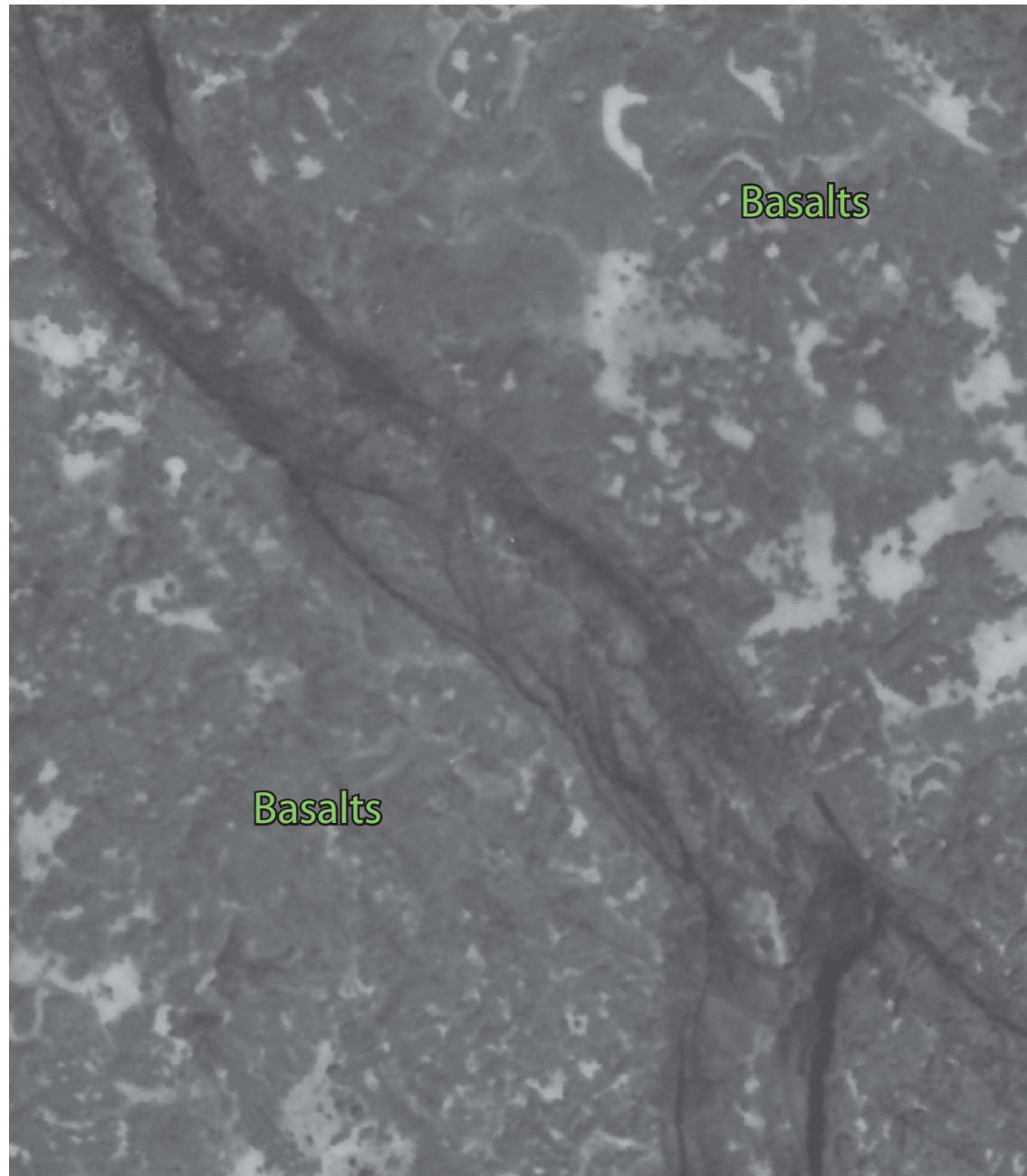
Aerial photography
1994



Quickbird image
2006



Aerial photography
1994



Quickbird image
2006

